The sign and value of the neutron mean squared intrinsic charge radius

Yu. A. Aleksandrov
Joint Institute for Nuclear Research, Dubna

Fiz. Élem. Chastits At. Yadra **30**, 72–122 (January–February 1999)

The connection between the neutron mean squared intrinsic charge radius $\langle r^2_{E,\text{in}}\rangle_N$ and the neutron–electron scattering length a_{ne} measured in low-energy neutron physics is discussed. Special attention is paid to the validity of the Foldy formula giving this connection. It is shown that there are two different ways of deriving the Foldy formula. A table is presented of the experimental data obtained during the period 1947–1997 which allow the determination of a_{ne}. These data split into two groups. One group leads to $\langle r^2_{E,\text{in}}\rangle_N>0$, and the other (including the Dubna data) to $\langle r^2_{E,\text{in}}\rangle_N<0$. The sources of possible systematic errors in the experiments are discussed. In particular, the effect of resonance nuclear scattering on the measured value of a_{ne} is studied. The experimental results on the measurement of a_{ne} in low-energy neutron physics are compared with the theory. It is shown that if the data leading to $\langle r^2_{E,\text{in}}\rangle_N>0$ are correct, then the modern theoretical ideas about the structure of the neutron (including the well developed Cloudy Bag Model) must be fundamentally changed. © *1999 American Institute of Physics.* [S1063-7796(99)00201-6]

INTRODUCTION

Studies of the neutron intrinsic charge radius $\langle r^2_{E,\text{in}}\rangle^{1/2}_N$ associated with the neutron–electron scattering length (interaction) a_{ne} have been carried out at low neutron energies since the mid-1960s at the I. M. Frank Neutron Physics Laboratory of the JINR. Such studies are at present the only reliable method of determining the value and sign of the intrinsic radius of the electric-charge distribution in the neutron, a fundamental characteristic which serves as an important and reliable test of the modern theoretical ideas about the neutron. The present accuracy of measurements in neutron physics (in contrast to high-energy electron scattering) allows conclusions to be drawn about the contribution to a_{ne} of a given radius. The author hopes that the present review will help to eliminate the doubts which sometimes arise in interpretations of the measurement results.

In Sec. 1 of this review we show that the relativistic vibration of particles subject to the Dirac equation is an unavoidable consequence of the Dirac theory. We study the approach proposed by Foldy to describing the electromagnetic structure of the neutron and the Foldy formula relating the experimentally measured neutron–electron scattering length a_{ne} to the neutron mean squared intrinsic charge radius $\langle r^2_{E,\text{in}}\rangle_N$.

In Sec. 2 we study the scattering of particles with internal structure, introduce the concept of form factors, and discuss their main properties, including their clear interpretation in the Breit coordinate frame, which at low energies coincides with the coordinate frame of a nucleon at rest.

In Sec. 3 we show that the Foldy formula can also be obtained by using the concept of form factors and the Sachs definition of the charge form factor of the nucleon. We conclude that the Foldy formula is valid and can be used for comparing experiment and theory.

Section 4 is devoted to experimental methods of studying the ne interaction. We review their history, beginning with the early studies of Fermi and Marshall in the 1940s. It is noted that two values of the neutron–electron scattering length were already known from neutron experiments by the end of the 1960s. One of these used with the Foldy formula gives a positive sign of $\langle r^2_{E,\text{in}}\rangle_N$, while the other gives a negative sign. The value $\langle r^2_{E,\text{in}}\rangle_N>0$ contradicted the theoretical static model of the neutron popular at that time. Then we study the method, proposed at the JINR Neutron Physics Laboratory (NPL), of measuring a_{ne} by means of neutron diffraction on a tungsten-186 single crystal. When this method is used, the measured ne effect becomes about 15 times stronger, and, as a result, a value $\langle r^2_{E,\text{in}}\rangle_N<0$ was obtained in the NPL experiments. We describe the transmission experiments mainly performed using a lead-208 sample by the Koester group (Garching, Germany) in collaboration with the NPL, by the Vienna–Oak Ridge group, and by physicists at the NPL. The results of the first two groups led to $\langle r^2_{E,\text{in}}\rangle_N>0$, while the Dubna experiments still prefer a value $\langle r^2_{E,\text{in}}\rangle_N<0$. We present a table giving the values of a_{ne} measured during the period 1947–1997.

In Sec. 5 we discuss the sources of possible systematic errors in the experiments mentioned above. One important source might be the effect of small-angle neutron scattering in transmission experiments for large distances between the sample and the detector.

Section 6 is devoted to the inclusion of the effect of inter-resonance interference on transmission experiments. It is pointed out that the effect of resonance scattering on the value found for a_{ne} can be neglected when a sample of ^{208}Pb or another even–even nucleus is used in the experiments. It is shown that in this case the results of the Koester group must lead to a value $\langle r^2_{E,\text{in}}\rangle_N<0$.

Finally, in Section 7 we compare the experimental results with the theoretical predictions and show that the modern theoretical ideas about the nucleon contradict the results

of the experiments leading to a positive sign of $\langle r^2_{E,\text{in}}\rangle_N$.

1. ZITTERBEWEGUNG

The relativistic Zitterbewegung of Dirac particles, i.e., particles with half-integer spin, sometimes called fermions, follows from the Dirac theory.[1] Actually, in the theory of velocity projection of, for example, a free electron or an electron in an electromagnetic field, the projection on the coordinate axes always has eigenvalues equal to the speed of light $\pm c$.

It would seem that measurement of the electron velocity projections must also always give $\pm c$. However, experimentally observed electrons usually have velocity less than c, and it might appear that there is a contradiction between theory and experiment. In fact, the theoretical velocity is the velocity at a particular instant of time, while the observed velocities are always averaged over some finite time interval.

Further theoretical study shows that the velocity projection on a coordinate axis consists of two parts: a constant part $c^2 p_1 H^{-1}$ and an oscillating part $\frac{1}{2}ic\hbar\alpha_1^0 \exp(-2iHt/\hbar)$, the frequency of which is $\omega = 2H/\hbar \geq 2mc^2/\hbar$. Here H is the relativistic Hamiltonian operator, p_1 is the particle momentum, and α_1^0 is given by $\alpha_1 = \alpha_1^0 \exp(-2iHt/\hbar)$, where α_m is the Dirac matrix. The constant part leads to the experimentally observed particle velocity v, while the part of the velocity oscillating with frequency of order $2mc^2/\hbar$ cannot be observed directly, because measurement gives the velocity averaged over a time interval significantly larger than the oscillation period $2\pi/\omega = \pi\hbar/(mc^2) \approx 4\times 10^{-21}$ sec. It is the oscillating part which makes the instantaneous theoretical velocity equal to $\pm c$.

The Zitterbewegung of a point Dirac particle with electric charge e (for example, an electron) causes the particle in the presence of an external magnetic field to behave as though it had a normal magnetic moment $e\hbar/2mc$ (in the case of a Dirac electron this is the Bohr magneton). This moment arises from the purely pointlike nature of the charge e and its vibration in a region of order $\hbar/mc \approx 4 \times 10^{-11}$ cm.

Another experimental phenomenon associated with the Zitterbewegung of a point charge e is, for example, the shift of the energy levels of the s electron in the hydrogen atom. The motion of a point charge resembles the motion of a charge distributed over a finite volume. In the Dirac theory this effect is described by the term proposed by Darwin in 1928.

It should be noted that in a recently published study[2] it is again stressed that Zitterbewegung is an ineluctable consequence of the Dirac theory.

An interesting type of interaction can exist between the neutron and the electron. It arises as a consequence of the meson theory of nuclear forces. Owing to the virtual dissociation of a neutron into a proton and a π^- meson, the neutron is surrounded by a meson cloud of size of order $\hbar/m_\pi c$, and an electric field can be expected to be present in the immediate vicinity of the neutron. When a neutron approaches an electron at fairly short distances, electrostatic interaction forces must arise between them. These forces will affect the neutron–electron scattering length a_{ne}.

Therefore, if a particle has an internal electromagnetic structure, the experimentally measured intrinsic charge and current density distribution will consist of an intrinsic part and an additional effect associated with the Zitterbewegung. Since it is the former which is of greatest interest, it is necessary to be able to separate these contributions.

More than 45 years ago, Feshbach showed[3] that in the scattering of electrons of energy of the order of several tens of MeV by a nucleus (more precisely, for $qR \ll 1$, where $q = 2k \sin\theta/2$ is the wave number of the recoil and R is the nuclear radius), the only measurable parameter indicating the nuclear size is the rms nuclear radius.

In the case of the scattering of very slow neutrons by atoms, a similar problem was apparently first solved by Fried,[4] and then later in more detail by Foldy[5] in the 1950s. Foldy showed that the experimentally measured interaction between the neutron and the electron, in particular, the neutron–electron scattering length a_{ne}, consists of two parts: a magnetic term containing the neutron anomalous magnetic moment, which can be calculated theoretically on the basis of the Zitterbewegung phenomenon, and an intrinsic term, which arises from the spatial distribution of the neutron electric charge due to the virtual dissociation of the neutron into a proton and a π^- meson.

The problem of neutron scattering on a weak, slowly varying, purely electrostatic potential $\varphi(r)$ was solved by Foldy on the basis of the following generalized Dirac equation:

$$\gamma_\mu\left(\frac{\partial\Psi}{\partial x_\mu}\right) + \frac{Mc}{\hbar}\Psi - \frac{1}{\hbar c}\sum_{m=0}^{\infty}\left[\varepsilon_m\gamma_\mu\cdot\Box^m A_\mu + \frac{1}{2}\mu_m\gamma_\mu\gamma_\nu\cdot\Box^m\left(\frac{\partial A_\mu}{\partial x_\nu} - \frac{\partial A_\nu}{\partial x_\mu}\right)\right] = 0, \tag{1}$$

where the electromagnetic field is described by the four-dimensional vector potential $A_\mu(x) \equiv A((r,t); i\varphi(r,t))$, $x \equiv (r,it)$, $\gamma_{\mu\nu}$ are the Dirac matrices, $\Box = \Delta - (1/c^2)\times(\partial^2/\partial t^2)$ is the d'Alembertian, and the coefficients ε_m and μ_m characterize the intrinsic electromagnetic structure of the neutron. In particular, ε_0 is the total electric charge of the neutron and μ_0 is the neutron anomalous magnetic moment. The other terms ($m = 1,2,3,\ldots$) describe the higher radial moments of the intrinsic electric charge distribution of the particle.

For $m = 0$, Eq. (1) reduces to the Dirac equation with electromagnetic potentials, the last two terms of which have the form

$$-\mu_n e\hbar/(2Mc)(\boldsymbol{\sigma}\mathbf{H}) - i\mu_n e\hbar/(2Mc)(\boldsymbol{\alpha}\mathbf{E}). \tag{2}$$

The first term, containing $\mathbf{H}$, is the interaction energy of the neutron magnetic moment $\mu_n e\hbar/2Mc$ and the magnetic field $\mathbf{H}$ and gives the magnetic interaction. The second term, called the Foldy interaction, arises from the Zitterbewegung of the neutron having magnetic moment $\mu_n e\hbar/2Mc$.

In the first Born approximation, Eq. (1) can be used to calculate the neutron–electron scattering length. At small momentum transfers only the terms with $m = 0$ and $m = 1$ are

important, and in the first Born approximation the amplitudes of ne scattering found from (1) have the form

$$f_0(\mathbf{k}) = -\frac{M\varepsilon_0}{2\pi\hbar^2}\int \exp(-i\mathbf{kr})\phi(\mathbf{r})d\mathbf{r}, \tag{3}$$

$$f_1(\mathbf{k}) = -\frac{M}{2\pi\hbar^2}\left[\varepsilon_1 + \frac{\hbar}{2Mc}\mu_0 + \frac{1}{2}\left(\frac{\hbar}{2Mc}\right)^2\varepsilon_0\right] \times \exp(-i\mathbf{kr})\nabla^2\varphi(\mathbf{r})d\mathbf{r}. \tag{4}$$

Since for the neutron $\varepsilon_0 = 0$ and $\mu_0 = \mu_n e\hbar/2Mc$, for $k \to 0$ the neutron–electron scattering length will take the form

$$a_{ne} = 2Me\varepsilon_1/(\hbar^2)[\varepsilon_1 + \mu_n e(\hbar/2Mc)^2]. \tag{5}$$

In this equation ε_1 describes the radial extent of the distribution of intrinsic electric charge in the neutron. The term containing μ_n is the Foldy contribution due to the Zitterbewegung of a particle with anomalous magnetic moment μ_n.

Weisskopf proposed an elegant derivation of Eq. (5) taking into account the neutron anomalous magnetic moment (see, for example, Ref. 6). The assumption that the neutron obeys the Dirac equation leads to the relativistic Zitterbewegung of a moving neutron. The neutron trajectory is a helix whose radius is of the order of the neutron Compton wavelength $R \simeq \hbar/Mc$. The neutron moves along the helix at the speed of light. The pitch of the helix is such that the translational motion of the neutron is characterized by the velocity v observed experimentally. If the neutron is located at a distance of order R from an electron (i.e., from a point charge), there is a magnetic spin–orbit interaction between the electron current and the neutron magnetic moment. This is the Foldy interaction, whose contribution to the scattering length is equal to the second term of (5).

The Foldy analysis is fundamentally phenomenological. The quantities ε and μ are introduced as coefficients whose values can be obtained only from experiment.

If e is the particle charge, we can introduce the various moments of the distribution of this charge:

$$\chi_n = \int r^{2n}\rho(\mathbf{r})dV = 4\pi\int r^{2n+2}\rho(r)dr, \tag{6}$$

where $\rho(r)$ is a spherically symmetric charge density [in the case of a uniformly smeared charge, $\rho = e/(\frac{4}{3}\pi R^3) = \text{const}$, where R is the particle radius] and $dV = 4\pi r^2 dr$ is the volume element.

The total charge of the system ($n = 0$) is $e = \int\rho(\mathbf{r})dV = 4\pi\int r^2\rho(r)dr$ (for the neutron, $e = 0$). In the Foldy study ε_1 is related to the second radial moment ($n = 1$) of the intrinsic electric charge distribution or to the mean squared intrinsic charge radius $\langle r^2_{E,\text{in}}\rangle$:

$$\varepsilon_1 \sim (1/6)\int r^2\rho_{\text{in}}(\mathbf{r})dV = (e/6)\langle r^2_{E,\text{in}}\rangle, \tag{7}$$

where $\rho_{\text{in}}(\mathbf{r})$ is the intrinsic electric charge density. Foldy writes that following ε_1 in (7), "we employ a correspondence symbol rather than an equal sign here, since there is some ambiguity in relating the relativistic coefficients to the physical extension of a static charge distribution. The indicated correspondence is perhaps the most reasonable one."

Using the equal sign in (7), from (5) we find for the neutron

$$\langle r^2_{E,\text{in}}\rangle_N = 3\hbar^2/(Me^2)(a_{ne} - a_F) \tag{8}$$

where $a_F = \mu_n e^2/2Mc^2 = -1.468\times 10^{-3}$ F is the scattering length corresponding to the Foldy interaction. Equation (8) can also be obtained by a different method, without using (7), but instead using the concept of form factors.

2. FORM FACTORS

It is well known that the structure of the ground state of an atom is usually understood to be the spatial distribution of the electrons in it and is described by the ground-state wave function. The electric charge density in the ground state, for example, of the hydrogen atom, at the point x is $e\rho(x)$, where $\rho(x)$ is the probability density of finding the electron at the point x.

In the case of nuclei, the electric charge distribution will no longer be identical to the nuclear mass distribution. Moreover, an additional difficulty arises in the case of an isolated nucleon. When a particle scatters on it, the nucleon undergoes a strong recoil, and it is practically impossible to calculate the electric charge distribution in the nucleon from the scattering data. Therefore, the structure of the nucleon and also of nuclei is described using form factors.

If the incident particle of charge ze and kinetic energy E and the target particle of charge Ze are spinless and do not possess structure (i.e., they are point particles), and the target particle does not undergo recoil, then in the Born approximation, where it is assumed that the incident and scattered particles can be described by plane waves (for $Zze^2/\hbar c \leqslant 1$), the nonrelativistic Rutherford expression gives the effective scattering differential cross section:

$$(d\sigma/d\Omega)_{\text{Ruth}} = z^2Z^2e^4/(16E^2\sin^4\theta/2). \tag{9}$$

If the target particle is not a point particle but has a spherically symmetric spatial density distribution, it can be shown that the expression for the effective scattering differential cross section is[7]

$$d\sigma/d\Omega = (d\sigma/d\Omega)_{\text{Ruth}}|F(q^2)|^2, \tag{10}$$

where $F(q^2)$ is the form factor and q^2 is the squared four-momentum transfer. Here $q^2 = (p_f - p_i)^2 = (p_{fe} - p_{ie})^2$, where p_i, p_f, p_{ie}, and p_{fe} are the initial and final four-momenta of the proton and electron. The spatial components of the four-momentum coincide with the particle momentum $\mathbf{p}$, and the time component is iE/c, where E is the particle energy.

In 1950 Rosenbluth obtained[8] a well known expression describing the differential cross section for the elastic scattering of an electron on a spin-1/2 particle of finite size, mass M, electric charge e, and anomalous magnetic moment μ_k:

$$d\sigma/d\Omega = (d\sigma/d\Omega)_0\{(F_1^2 - (q/2Mc)^2[2(F_1 + \mu_K F_2)^2\tan^2(\varphi/2) + \mu_K^2 F_2^2]\}, \tag{11}$$

where $(d\sigma/d\Omega)_0$ is the differential cross section for electron elastic scattering on a point charge [since the particles have nonzero spin, $(d\sigma/d\Omega)_0 \neq (d\sigma/d\Omega)_{\text{Ruth}}$], $F_1(q^2)$ is the Dirac form factor describing the spatial charge distribution and the associated normal magnetic moment, $F_2(q^2)$ is the Pauli form factor associated with the spatial distribution of the anomalous magnetic moment, and q^2 is the squared four-momentum transfer. The functions F_1 and F_2 have a clear physical interpretation.

Later, in 1962 Sachs[9] derived linear combinations of the form factors F_1 and F_2 convenient for working with experimental data. These are the charge form factor

$$G_E(q^2)=F_1(q^2)+\mu_K(q\hbar/2Mc)^2F_2(q^2) \tag{12}$$

and the magnetic form factor

$$G_M(q^2)=F_1(q^2)+\mu_K F_2(q^2). \tag{13}$$

Since (12) and (13) are linear combinations of F_1 and F_2, it is impossible to show which set is more fundamental, F_i or G_i. However, the Rosenbluth expression is written more simply in terms of the G_i than the F_i, as in the former there is no cross term involving G_E and G_M like F_1F_2 [see (11)]. Moreover, the combination of form factors F_1 and F_2 is chosen so that the complete electric and magnetic parts are separated. Therefore, G_E and G_M describe the distribution of the total charge and the total magnetic moment. The experimental data for $G_{EN}(q^2)$ of the neutron obtained from electron–deuteron scattering are shown in Fig. 1, taken from Ref. 10. We see that G_{EN} is close to zero.

Although to describe observed phenomena it is sufficient to introduce the form factors as phenomenological functions of the squared momentum transfer, it is useful for purely illustrative purposes to have a clear interpretation of them. This is possible in the Breit coordinate frame, which corresponds to the requirement that the spatial components of the four-vector p_i+p_f be zero. In this frame the three-momenta of the initial and final protons are equal in magnitude and opposite in direction, and the corresponding energies are the same. In the Breit frame the form factor G_E is interpreted as the Fourier transform of the spatial distribution of the electric charge density

$$\rho(\mathbf{r})=e/(2\pi)^3\int G_E(q^2)\exp(-i\mathbf{qr})d\mathbf{q} \tag{14}$$

or

$$G_E(q^2)=1/e\int \rho(\mathbf{r})\exp(i\mathbf{qr})d\mathbf{r}. \tag{15}$$

Here we can speak of the spatial image of the neutron, i.e., its electromagnetic structure. If $G_E(q^2)=\text{const}$, it follows from (14) that $\rho(r)\sim e\delta(r)$, where $\delta(r)$ is the delta function. The q^2 dependence of G_E characterizes the deviation of the charge distribution from a point distribution. However, $\rho(r)$ is not a function specified in a fixed coordinate system. Each value of q corresponds to a particular reference frame, and so the spatial structure of the nucleon specified by (14) and (15) is, in general, rather complicated. It becomes a well defined charge distribution only in the nonrelativistic case of small momentum transfers ($\hbar^2q^2 \ll M^2c^2$), when the change of energy of the nucleon at rest can be neglected. In this case the Breit system coincides with the coordinate system of a nucleon at rest, and the form factor G_E has a clear interpretation as the Fourier transform of the spatial distribution of the total electric charge density. Since the total charge of a particle is $Q=\int\rho(\mathbf{r})d\mathbf{r}$, from (14) we find that $Q=eG_E(0)$. For the proton $G_{EP}(0)=1$ and $F_{1P}(0)=1$, and for the neutron $G_{EN}(0)=0$ and $F_{1N}(0)=0$. If the particle has no charge, this only implies that $G_E(0)=0$. Such a particle can emit virtual photons and possesses a charge distribution. A particle is truly neutral when the form factors are zero for all q^2.

In the limiting case of low energies (small momentum transfers), Eq. (15) can be expanded in a series in powers of q^2. Normalizing $\rho(r)$ by the condition $\int\rho(r)4\pi r^2dr=e$, we obtain $G_E(q^2)=1-\frac{1}{6}\langle r_E^2\rangle q^2+\ldots$, and the particle size is characterized by the mean squared radius of the total electric charge distribution:

$$\langle r_E^2\rangle=1/(e)\int\rho(\mathbf{r})4\pi r^2dr=6(dG_E/dq^2)_{q^2=0} \tag{16}$$

or

$$\langle r_E^2\rangle=6(dF_1/dq^2)_{q^2=0}+3/2\mu_k(\hbar/Mc)^2. \tag{17}$$

The second term in (17) is a consequence of the Zitterbewegung of a particle with anomalous magnetic moment μ_k and obeying the Dirac equation (the Foldy term). The first term in (17) arises because the nucleon has internal structure and is related to the behavior of the Dirac form factor as a function of q^2. Using $\langle r_{E,\text{in}}^2\rangle_N$ to denote the mean squared electric radius associated with the internal structure of the nucleon, also called the Dirac radius, we can write

$$\langle r^2{}_{E,\text{in}}\rangle_N=6(dF_1/dq^2)_{q^2=0}. \tag{18}$$

From (17) and (18) it follows that the total mean squared electric radius of the particle is

$$\langle r_E^2\rangle=\langle r_{E,\text{in}}^2\rangle+\langle r_F^2\rangle, \tag{19}$$

where $\langle r_F^2\rangle=\frac{3}{2}\mu_k(\hbar/Mc)^2$ is the Foldy term. For the proton $\langle r_F^2\rangle_P=0.1189\,\text{F}^2$, and for the neutron $\langle r_F^2\rangle_N=-0.1268\,\text{F}^2$.

We note that the sign of the mean squared electric radius of a neutral (uncharged) particle can in principle be either positive or negative. In the absence of the Foldy term (for example, in static models of the nucleon, when $M\to\infty$; see below), for the neutron the sign of $\langle r_E^2\rangle=\langle r_{E,\text{in}}^2\rangle$ is determined by the sign of the charge located at the periphery. Since that charge is a π^- meson, the sign of $\langle r_E^2\rangle$ must be negative.

Using (16)–(18), and (8), we find that

$$(dG_E/dq^2)_{q^2=0}=14.41a_{ne}, \tag{20}$$

where a_{ne} is in F. Therefore, the study of ne scattering gives information about the derivative $(dG_E/dq^2)_{q^2=0}$. Analogous information on $(dG_E/dq^2)_{q^2=0}$ (and also on $\langle r_{E,\text{in}}^2\rangle$) can also be obtained from electron–deuteron scattering experiments (see Fig. 1), but the experimental errors make this insufficiently accurate.

It is sometimes convenient to deal with the isoscalar G_E^S and isovector G_E^V combinations of G_E:

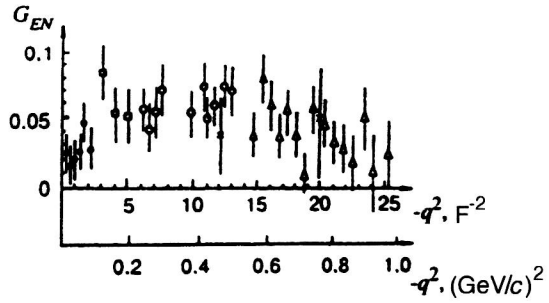

FIG. 1. Experimental dependence of the neutron charge form factor on q^2. Experiments on elastic ed scattering.

$$G_E = G_E^S + \tau_Z G_E^V, \tag{21}$$

where $\tau_z = 1$ for the proton and $\tau_z = -1$ for the neutron. Then from (21) for the neutron we find

$$G_{EN} = G_E^S - G_E^V, \tag{22}$$

while for the proton

$$G_{EP} = G_E^S + G_E^V. \tag{23}$$

Since G_{EN} is close to zero (see Fig. 1), we have

$$G_E^S \approx G_E^V. \tag{24}$$

3. THE FOLDY FORMULA

Let us now derive (8) without using Eq. (7), about which doubts have recently been expressed (see, for example, Ref. 11). Equation (7) relates the sign of the equality between the parameter ε_1 introduced by Foldy and the mean squared charge radius of the neutron. We use Eqs. (17) and (18), about which there is apparently no doubt at low energies.

We assume that the mass of the colliding particle (electron) is much smaller than the nucleon mass and that the nucleon is at rest before and after the collision. We also assume that the nucleon electric charge density is spherically symmetric. Then the potential energy of the interaction between the electron and the nucleon at the point r where the electron is located will involve contributions from all parts of the nucleon:

$$U(r) = -e^2 \int \frac{\rho(r'')dV''}{|r''-r|}, \tag{25}$$

where $|r''-r|$ is the distance from the point r'' where the charge $\rho(r'')dV$ is located to the observation point r.

Substituting $U(r)$ into the expression for the Born approximation of the scattering amplitude,

$$f(\varphi) = -M/(2\pi\hbar^2) \int U(\mathbf{r}) \exp(i\mathbf{kr}) dV, \tag{26}$$

where $\mathbf{K} = k|\mathbf{n}_0 - \mathbf{n}|$, $\mathbf{n}_0$ is the unit vector in the direction of the incident beam, and $\mathbf{n}$ is the unit vector in the direction of $\mathbf{r}$, so that $K = 2k \sin \varphi/2$, we find the electron–neutron scattering length a_{ne}:

$$a_{ne} = Me^2/(2\pi\hbar^2) \int \exp(i\mathbf{Kr}) dV \times \int \rho(r'')/(|r''-r|) dV''. \tag{27}$$

Performing the calculations (see, for example, Refs. 5 and 12), we obtain

$$a_{ne} = 8\pi M(e/\hbar k)^2 \int \sin Kr/(Kr) \rho(r) r^2 dr, \tag{28}$$

or for small Kr, since $\langle r_E^2 \rangle = 4\pi/(e) \int \rho(r) r^4 dr$ is equal to the sum of two terms [see (17) and (18)], while for the neutron $4\pi \int \rho(r) r^2 dr = 0$,

$$a_{ne} = 2Me/(\hbar^2)[e/(6)\langle r_{E,\text{in}}^2 \rangle_N + \mu_n e(\hbar/(2Mc))^2], \tag{29}$$

from which Eq. (8) follows directly. Comparing (5) and (29), we see that $\varepsilon_1 = \frac{1}{6} e \langle r_{E,\text{in}}^2 \rangle_N$, i.e., we have an equality and not a proportionality. This conclusion essentially follows from the Sachs definition of the charge form factor G_E [see (12)]. Therefore, Eq. (7) introduced by Foldy and taken with the equality is valid and can be used to compare experiment and theory.

We also note that information on $\langle r_{E,\text{in}}^2 \rangle_N$ can be obtained if the experimental dependence $G_{EN}(q^2)$ is known (for example, from experiments on electron–nucleon scattering). However, the measurement errors existing at present do not permit this for the case of the neutron (see Fig. 1).

4. EXPERIMENTAL METHODS OF STUDYING THE *ne* INTERACTION

The first attempts to observe ne scattering were made in 1932, but more accurate measurements of a_{ne}, begun by Fermi, were made only in the mid-1940s and later. They are largely based on either observation of the asymmetry of the scattering of thermal neutrons by atoms, or study of the energy dependence of the total cross section for neutron interactions with atoms at energies of eV. Using Eq. (8), the magnitude and sign of $\langle r_{E,\text{in}}^2 \rangle_N$ can be obtained from the measured value of a_{ne}. However, since a_{ne} and a_F are quantities of the same order of magnitude, very precise measurements are needed to find $\langle r_{E,\text{in}}^2 \rangle_N$. Such measurements are possible by studying the interaction of low-energy neutrons with heavy atoms. The differential cross section for the coherent scattering of slow neutrons with wavelength of the order of the atomic size by atoms is given by

$$\sigma(\theta) = |a + Zf(\sin\theta/\lambda) a_{ne}|^2, \tag{30}$$

where a is the coherent nuclear scattering length, $\theta = \varphi/2$, φ is the scattering angle, and $f(\sin\theta/\lambda)$ is the atomic form factor. Estimates show that the ratio of the second term to the first is about 1% for heavy atoms, and so a_{ne} can be measured.

There are two old methods of studying the ne interaction. One of them,[13] first used by Fermi and Marshall in 1947, is based on the observation of the very small asymmetry of thermal-neutron scattering due to the θ dependence of f. Thermal neutrons have a wavelength of about 2 Å, which

is at least 10^4 times larger than the nuclear size. Consequently, thermal neutrons must undergo spherically symmetric scattering by nuclei in the c.m. frame. Deviations from the scattering symmetry can arise from not only the ne interaction, but also, for example, from the interaction of the magnetic field produced by the electron currents inside the atom with the neutron magnetic moment. Effects of this type can be avoided by using atoms whose shells are all filled. There may also be other factors leading to asymmetry of the scattering: the interference of waves scattered by different atoms, thermal oscillations of the atoms, and so on. In the study by Fermi and Marshall and in other similar experiments, the scattering of thermal neutrons having a Maxwell velocity distribution was observed at the angles $\varphi=45°$ and 135°. In order to avoid the effects of magnetic scattering and molecular diffraction, monatomic noble gases with filled electron shells, in particular, xenon ($Z=54$), were used as the scatterer. The difference between $f(45°)=0.78$ and $f(135°)=0.52$ specifies the asymmetry of the ne scattering manifested in the background of the strong isotropic nuclear scattering. The measured value of the asymmetry must be corrected for the difference in the geometrical parameters of the detectors, and the asymmetry due to the thermal motion of the gas atoms, which is several times greater than the measured effect, must be taken into account. In the first approximation, no magnetic scattering is expected in neutron scattering for atoms with filled electron shells. In the second approximation the effect of the interaction of the neutron magnetic moment with the currents arising in virtual excited states of the noble-gas atom should be seen. This type of effect was studied by Fermi and Marshall, who showed that it makes up a very small fraction of the principal ne interaction.

The effect of Schwinger scattering was also studied. Estimates showed that it is also negligible, because Schwinger scattering is associated with spin and practically does not interfere with nuclear scattering if the neutrons are unpolarized. The main defect of the experiments is the need to introduce a large correction for the effect due to the thermal motion of the gas atoms. The main contribution to this correction comes from neutrons having large wavelength right in the region where deviations from the Maxwell distribution can be expected. This can lead to incorrect calculation of the correction. In the most accurate experiments the correction was determined experimentally on the basis of measurements using argon and neon, for which ne scattering is insignificant.

It should be borne in mind that even in experiments with monatomic gases, it is possible to have a small scattering asymmetry associated with the interference of waves scattered by different atoms of the gas. This was pointed out by Akhiezer and Pomeranchuk.[14] The interference arises from correlations between the relative locations of the atoms, because the distance between the centers of two neighboring atoms cannot be smaller than twice the atomic radius. The calculations showed that the ratio of the intensities of neutrons scattered at angles φ_1 and φ_2 is given by

$$\varepsilon=\frac{1+4\pi(2R)nf(\varphi_1)}{1+4\pi(2R)nf(\varphi_2)}, \tag{31}$$

where $f(\varphi)=\cos\eta/\eta^2-\sin\eta/\eta^3$, $\eta=(8\pi R/\lambda)\sin(\varphi/2)$, R is the atomic radius, and n is the gas density. Calculations using (31) showed that when the gas is at atmospheric pressure, the interference correction is only 3.5% of the measured ne-interaction effect.

Krohn and Ringo[15] performed precision measurements using the Fermi–Marshall method at Argonne in 1965–1973. The measurements were made for xenon, krypton, and argon, and neon was used to check the correctness of the calculation for the scattering asymmetry due to the thermal motion of the gas. The value of this correction exceeded the desired effect by a factor of 4 for xenon, 10 for krypton, and 18 for argon. In second order in a_{ne}/a from (30) we find

$$R=1+8\pi(aa_{ne}/\sigma_{sc})Z\Delta f(1+\delta), \tag{32}$$

where $R=\sigma(\varphi_1)/\sigma(\varphi_2)$ is the measured scattering asymmetry taking into account corrections; $a=\Sigma a_j n_j$; a_j is the nuclear scattering length of the jth nuclide; n_j is the concentration of the jth nuclide in the isotopic mixture; σ_{sc} is the scattering cross section; $\Delta f=\langle f(\theta_1)-f(\theta_2)\rangle$ is the difference of the atomic form factors averaged over the neutron spectrum; $\varphi_1=2\theta_1=45°$; $\varphi_2=2\theta_2=135°$; and

$$\delta=\frac{a_{ne}}{2a\Delta f}\langle f^2(\theta_1)-f^2(\theta_2)\rangle-\frac{8\pi aa_{ne}}{\sigma_{sc}}\langle f(\theta_2)\rangle. \tag{33}$$

The scattering lengths a for xenon and krypton were determined by measuring the critical angles of total neutron reflection from the surface of the liquified gases; in addition, the value of a for xenon was obtained from experiments on neutron diffraction on XeF_4. The scattering cross sections of the noble gases were measured in special experiments using the cross section for scattering on neon as the standard. Special measures were taken to purify the gases from admixtures, particularly of light gases, since even small admixtures can strongly distort the experimental results. The measurements were carried out at various pressures of the scattering gas. No changes in the scattering asymmetry were observed within the error as the pressure varied from 0.4 to 1.2 atm. As a result, after the introduction of the correction for Schwinger scattering it was found that

$$a_{ne}=(-1.33\pm0.03)\times10^{-3}\,\text{F}. \tag{34}$$

Reasons for possible additional systematic errors might be the following.

(1) A very small observable scattering asymmetry in the background of the strong symmetric nuclear scattering (in Ref. 15 this was only 0.5% and was measured with an error of ±2.5%).

(2) Spurious effects which are not completely eliminated, for example, effects due to the presence of unknown neutron p-wave resonances (with width of order 10^{-8} eV), admixtures of light gases, and so on.

(3) The large introduced correction for the scattering asymmetry due to the thermal motion of the gas (for xenon this is four times larger than the studied effect).

As an example, let us estimate the scattering asymmetry of thermal neutrons due to the possible presence of a weak p-wave resonance in xenon near neutron energies of order 0.1 eV. The scattering amplitude due to this p resonance in the region of thermal energies where potential p scattering is unimportant has the form[16]

$$f_p \approx \frac{3\Gamma_n(E-E_0)}{2k[(E-E_0)^2+\Gamma^2/4]}\cos\varphi, \tag{35}$$

where $\Gamma_n=\Gamma_n^0(kR)^2E^{1/2}$. The value of Γ_n^0 can be estimated from the expected value of the p-wave strength function of xenon, $\Gamma_n^0/D\approx 2\times 10^{-4}$ (Ref. 17). This value leads to $\Gamma_n\approx 1.42\times 10^{-9}$ eV and $f_p\approx 4.1\times 10^{-4}$ F, which in turn allows the false forward–backward scattering asymmetry to be estimated as $[(b_{\rm coh}+f_p\cos\varphi_1)/(b_{\rm coh}+f_p\cos\varphi_2)]^2-1=2\times 10^{-4}$. The corresponding quantity due to ne scattering is 60×10^{-4}, and the error quoted in Ref. 15 in the determination of a_{ne} must be at least doubled. In reality, the situation may be much more serious, because Γ_n^0 can exceed the value that we quote by several times. We note that a resonance with a neutron width even of order 10^{-7} eV could not really have been observed in the total cross section up to the present time in the usual experiments using the transmission method. Special searches for weak p-wave resonances show that resonances with neutron widths of 10^{-7} eV are found only for sample thickness $\geq 10^{23}$ nuclei/cm^3, which is attainable for gaseous xenon in samples $\sim$1 m long at a pressure of order 50 atm.

The second method was first used by Havens, Rabi, and Reinwater.[18] It consists of observing the dependence of the total scattering cross section on the neutron wavelength near $\lambda\approx 1$ Å ($E\approx 0.08$ eV). The nuclear scattering length must remain constant, while the atomic form factor is what causes the total cross section to vary as a function of λ. Liquid lead and bismuth were used as the scatterers. The total cross section was measured in the range $\lambda=0.3-1.3$ Å. In this range of wavelengths the change of the total cross section due to the ne interaction is 0.1 b. Corrections for other effects must be introduced. For example, the correction for interatomic interference amounts to 0.2 b in this wavelength range. It is also necessary to introduce a correction for the relative velocity due to the thermal motion of the target atoms, and also to take into account the effect of neutron capture in the material studied and on impurities. It was later shown[19] that corrections for the aggregate state of the matter at neutron energies below 1 eV can be introduced, as a rule, only with large uncertainties. Therefore, despite the high statistical accuracy of the method, the overall accuracy is apparently not very good. The most accurate value obtained by this method at neutron energies below 1 eV,

$$a_{ne}=(-1.56\pm 0.05)\times 10^{-3}\ \text{F}, \tag{36}$$

was found by Melkonian *et al.*[20] in 1959.

Therefore, already by the end of the 1960s two values of the scattering length a_{ne} were known from experiments. By that time the Foldy formula (8) relating the ne effect to the neutron intrinsic charge radius was also known. According to this formula, the first value of a_{ne} [see (34)] gives $\langle r^2_{E,\rm in}\rangle_N>0$, while the second [see (36)] gives $\langle r^2_{E,\rm in}\rangle_N<0$. By the same time Chew and Low had formulated the ideas of Yukawa mathematically, and had obtained a satisfactory quantitative interpretation of the experiments on π-meson photoproduction[21] and also on low-energy ($E\ll Mc^2=0.95$ GeV) scattering.[22] The proton and neutron magnetic moments had also been calculated approximately.[23,24] In the Chew–Low theory the nucleon is treated as an extended source of the virtual meson field. The virtual process $n\to p+\pi^-$ gave a negative tail, i.e., an external pion cloud of the neutron electric charge distribution, with a characteristic size $\hbar/m_\pi c=1.4$ F. The nucleon was assumed to be infinitely heavy, so that in the first approximation the recoil in virtual processes could be neglected. A static model of this type must lead to a negative value of the neutron squared intrinsic charge radius. Therefore, the value $a_{ne}=-1.33(3)\times 10^{-3}$ F (34) contradicted theory, while the value $a_{ne}=-1.56(5)\times 10^{-3}$ F (36) agreed with it. At that time the intrinsic structure of the nucleon was not really understood, and the nucleon properties could not be calculated. Only 20 years later did the quark representation of the nucleon clear up the situation: the nucleon is a bag containing three quarks.

The third experimental method of studying the ne interaction was the method of cancellation of the nuclear scattering lengths in neutron reflection from a mirror. This was the method used by Hughes *et al.*[25] It is well known that the index of refraction of matter for neutrons of wavelength λ is related to the coherent scattering length as (in the absence of magnetic scattering of neutrons)

$$n^2=1-(\lambda^2/\pi)\sum a_jN_j, \tag{37}$$

where N_j is the number of particles of type j in 1 cm^3 of matter, and a_j is the coherent scattering length for neutron scattering by particles of type j. For the precision determination of the index of refraction of two materials, one measures the critical angle $\varphi_{\rm cr}$ of total reflection at the boundary:

$$\varphi_{\rm cr}^2=n_A^2-n_B^2 \quad (\text{for } \varphi_{\rm cr}\ll 1), \tag{38}$$

where n_A and n_B are the indices of refraction of the two materials.

For the liquid oxygen and bismuth used in Ref. 25, Eqs. (37) and (38) give

$$(\pi/\lambda^2)\varphi_{\rm cr}^2=N_{\rm Bi}a_{\rm Bi}\left(\frac{N_{\rm O}a_{\rm O}}{N_{\rm Bi}a_{\rm Bi}}-1\right)-N_{\rm O}Z_{\rm O}a_{ne}\left(\frac{N_{\rm Bi}Z_{\rm Bi}}{N_{\rm O}Z_{\rm O}}-1\right) \tag{39}$$

[since we are dealing with small-angle (forward) scattering, the atomic form factor is unity]. We have the ratio $N_{\rm O}a_{\rm O}/N_{\rm Bi}a_{\rm Bi}=1.024$, while $N_{\rm Bi}Z_{\rm Bi}/N_{\rm O}Z_{\rm O}\approx 7$. Therefore, the measured value of the critical angle $\varphi_{\rm cr}$ is roughly equally determined by the uncancelled nuclear scattering and the ne interaction. This angle amounts to several minutes. The scattering lengths $a_{\rm O}$ and $a_{\rm Bi}$ (or, more precisely, $a_{\rm Bi}$ and the ratio $a_{\rm O}/a_{\rm Bi}$) were determined experimentally by measuring the scattering cross section of free atoms at a neutron energy of order 10 eV. The ne interaction is not manifested at this energy, because the form factor is practically

zero. To change over to the coherent scattering lengths a_O and a_{Bi} it is necessary to determine the cross section for the incoherent scattering of bismuth. This was done by additional experiments using long-wavelength neutrons, where only incoherent scattering occurs.

The critical angle measured experimentally[25] turned out to be 3.66 angular minutes. As a result, it was found that

$$a_{ne}=(-1.39\pm0.13)\times10^{-3}\,\mathrm{F}. \tag{40}$$

The mirror-reflection method has the advantage over other methods that the measured effect is to a large degree determined by the ne interaction itself. However, the final result of the Hughes experiment is based on the assumption that at energies ranging from 10 eV to the thermal length, the scattering unrelated to the ne interaction does not change. However, as pointed out by Halpern,[26] at energies of order 10 eV significant inelastic scattering can occur on bismuth and oxygen atoms. If this is so, then the values of a_O and a_{Bi} will differ from the values used in Ref. 25, which accordingly changes the final experimental results. There is also the problem of ensuring that there is no resonance effect in this energy range.

Since the desired ne effect amounts to only about 1% in the most accurate experiments, it would be very interesting to find a method in which the measured effect is more significant, as in the Hughes experiments. In the earlier studies there is always the danger of some unforeseen effect influencing the results. For example, when the method of measuring the total cross section for liquid lead or bismuth at energies from 0 to 10 eV is used, a change of the nuclear scattering cross section by only 0.1% leads to a 10% change in the desired ne scattering amplitude.

It follows from (30) that the relative value of the additional contribution to the scattering cross section is given by $\Delta\sigma_{ne}/\sigma=2Z\Delta f a_{ne}/a$. In the experiments based on the Fermi–Marshall method, Δf was only 0.26. Since the form factor is a function of the ratio $\sin\theta/\lambda$, to increase Δf it is necessary to perform measurements at smaller λ, while remaining at angles of less than 45°, or to perform a time-of-flight experiment for fixed angle θ in a wide range of λ. Moreover and even more important, it is necessary to find a nucleus with a very small value of the nuclear scattering length suitable for the measurements. Accordingly, searches for a heavy nucleus with small nuclear scattering length were undertaken at the JINR Neutron Physics Laboratory in 1965–1966. Such a nucleus was found, first theoretically and then experimentally. It turned out to be tungsten-186, whose nuclear scattering length for neutrons of energy ranging from zero to several eV is small (roughly ten times smaller than for naturally occurring tungsten), owing to the interference of potential and resonance scattering. It has the form[27]

$$a=R-\frac{\beta\Gamma_n}{2k_0E_0}\left(1+\frac{E}{E_0}\right)+a_{ne}Zf\left(\frac{\sin\theta}{\lambda}\right), \tag{41}$$

where Γ_n is the neutron width of the first resonance ($E_0=18.83$ eV) of ^{186}W; R takes into account potential scattering, the contribution of impurities, and also the insignificant contribution from other tungsten resonances; and β is the content of the ^{186}W isotope in the mixture. The results of the search were first presented[27] at the Seminar on Electromagnetic Interactions in Nuclear Reactions in 1966 at Dubna, and were then later published in Ref. 28. In Ref. 27 it was suggested that a single crystal of ^{186}W be used to measure the ne interaction by studying neutron diffraction in this crystal. In this way it was possible to increase the measured ne effect up to a few tens of percent. By varying the ^{186}W concentration in the mixture, it is possible to change the absolute value and sign of the scattering length.

Precision measurements of the neutron scattering length in scattering by a mixture of tungsten isotopes containing 90.7% ^{186}W were performed in a beam of cold neutrons ($\lambda\approx15$ Å) using the method of Christiansen filters.[29] The Christiansen filter, a vertical cavity between glass plates which is filled with a powder of the material under study, was placed in a well collimated neutron beam (the spread in the horizontal plane was less than 2–3′). The thickness of the cavity in the beam direction is several millimeters, and the cavity is wide enough to completely overlap the beam. The space between the powder grains is alternately filled with different liquids with known neutron index of refraction. Several meters behind the filter on the beam axis is a detector of width such that it can record neutrons scattered by the filter at angles of up to ~0.5° in the horizontal plane. The measurements consisted of observing the intensity of the small-angle scattering of the neutrons by the filter at several values of the liquid index of refraction (for example, for different mixtures of heavy $[Na_{D_2O}=(63.399\pm0.005)\times10^9\,\mathrm{cm}^{-2}]$ and light $[Na_{H_2O}=(-5.61\pm0.03)\times10^9\,\mathrm{cm}^{-2}]$ water). The spread of the beam due to small-angle scattering is proportional to λ/a_0, where a_0 is the powder grain size. In principle, small-angle scattering should be completely absent when the liquid index of refraction n_L is equal to the powder index of refraction n_P, and appears when this condition is violated. In some range of n_L the scattering intensity is $I\sim(n_P-n_L)^2\approx[(Na)_L-(Na)_P]^2$. To record only scattered neutrons, a cadmium absorber was placed in front of the detector. It completely covers the incident beam and does not interfere with neutrons scattered at small angles. The absence of small-angle scattering implies that $(Na)_L=(Na)_P$, which gives the unknown value of a_P. These measurements gave[30] $a=(-0.466\pm0.006)$ F for the coherent scattering length of the tungsten powder (90.7% ^{186}W).

The neutronography experiments were carried out using two single-crystal spheres of diameter 5 mm composed of two different isotope mixtures. One contained 90.7% ^{186}W ($a=-0.466$ F), and the other ($a=+0.267$ F) was prepared from the first mixture with the addition of 14% natural tungsten. The principal measurements[31] were performed in 1968–9 and 1973 at setups at the stationary reactor of a branch of the Karpov Physico–Chemical Institute. Crystal monochromators were used to extract neutrons of wavelength $\lambda=1.17$ Å. The monochromator of one of the setups was a copper crystal with mosaic angle ≈40′. A (331) reflection was used. The grazing angle of the monochromator was $\theta_M=45°$, and the aperature angle of the first collimator was $\alpha_0=30'$. The admixture of neutrons with wavelength

$\lambda/2$ was less than 5%, $\Delta\lambda/\lambda \approx 2\%$. After reflection from the monochromator, the beam passed through a steel collimator with aperature angle $\alpha_1 = 40'$ and fell upon the studied single crystal. The mosaic angle of the single crystal was about 40′. The neutrons diffracted by the single crystal were recorded by a proportional counter filled with ^{3}He at a pressure of 10 atm. The counter was located at a distance of 40 cm from the sample and had a collimation window of area $20 \times 30\,\text{mm}^2$. All the measurements were performed using the $\theta - 2\theta$ technique. The detector aperature and the dimensions of the collimation system were chosen so that the total integrated intensity could be measured at all reflections. The degree to which this was satisfied was monitored. For this, the dimensions of the beam reflected from the crystal were determined for forward and backward reflections. These dimensions proved to be significantly smaller than the angular aperature of the detector in both the horizontal and the vertical directions. Possible shifting of the reflected beam with respect to the detector window as the sample and detector were moved was also studied experimentally. It was found that such shifts were less than a few millimeters, and so no part of the reflected beam could miss the detector window. The correctness of the measurements of the total integrated intensities of the reflections was confirmed by the agreement between the angular dependence of these intensities and the results of analogous measurements made using a second setup with the following parameters: a Pb monochromator for (110) reflection, $\lambda = 1.145$ Å, $\theta_M = 11°$, $\alpha_0 \approx 2.5°$, $\alpha_1 \approx 30'$, and also at the diffractometer of the Leningrad Nuclear Physics Institute. These setups differed greatly in their parameters, but the results of the measurements completely coincided.

The integrated intensities $I_{(hkl)}$ of eight reflections were measured at fixed wavelength: (110), (200), (220), (310), (400), (330), (420), and (510). Since tungsten is paramagnetic, it was expected that magnetic scattering would not contribute to the Bragg reflections, and the integrated intensity of the diffraction peak should be[31]

$$I_{(hkl)} = C(a + Zfa_{ne})^2 A_{(hkl)} \frac{\exp[-2B(\sin\theta/\lambda)^2]}{\sin 2\theta}, \quad (42)$$

where C is a constant, $A_{(hkl)}$ is the absorption factor, $\exp[-2B(\sin\theta/\lambda)^2]$ is the Debye–Waller factor taking into account the thermal vibrations of the atoms, and θ is the Bragg angle. The absorption factor was calculated, and it changed by no more than 4% in going from (110) to (510) reflection. Since the data on the value of B for tungsten available in the literature are very contradictory, attempts were made to calculate this factor and also to determine it experimentally. The calculations were performed using information about the specific heat of tungsten and its phonon spectrum. They gave $B = 0.162$ Å^2 and $B = 0.167$ Å^2 (Ref. 32). The measurements of B were performed using the same monochromator as for the neutronograms of the ^{186}W single-crystal spheres. The technique consisted of analyzing the angular dependence of the integrated intensity of the diffraction peaks appearing in the scattering of neutrons on compressed powder of naturally occurring tungsten. These measurements, performed at $T = 293$ K, gave $B = 0.19 \pm 0.02$ Å^2. In addition, the integrated intensities of the diffraction peaks were measured at the temperatures $T = 293$ and 80 K by the time-of-flight method at the pulsed IBR-30 reactor at the JINR. The measurements using compressed powder of naturally occurring tungsten gave $B = 0.17 \pm 0.02$ Å^2, and those with a cylindrical single crystal of ^{186}W gave $B = 0.15 \pm 0.01$ Å^2. The value $B = 0.17$ Å^2 was then used for processing the measurement results.

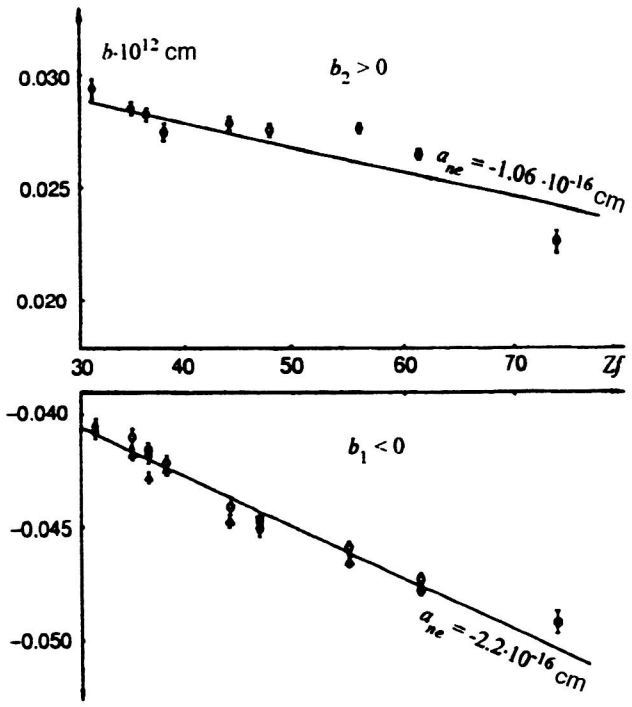

FIG. 2. Experimental dependence of the neutron coherent scattering lengths on Zf for two different isotope mixtures of tungsten.

It follows from (42) that the Zf dependence

$$\left(I_{(hkl)} \frac{\sin 2\theta \exp[2B(\sin\theta/\lambda)^2]}{A_{hkl}C}\right)^{1/2} = a + Zfa_{ne} \quad (43)$$

must be linear, and the slope of the line is a_{ne}. However, the experimental data[31] indicated that it is impossible to describe these data for two different tungsten isotope mixtures by a single value of a_{ne} (see Fig. 2). The values of a_{ne} differ by roughly a factor of two. More detailed study shows that this description of the results by a linear function is completely unsatisfactory ($\chi^2 \approx 65$). Possible reasons for this were studied, in particular, the effects of extinction and diffuse thermal scattering (DTS). The extinction effect can be neglected, owing to the small scattering cross section, because the known criterion for a thin crystal[33] in our case is exceeded by 250 times. Calculations showed that the DTS contribution to the diffraction peaks is less than 1.5%. In addition, it is known that the DTS contribution is proportional to the sample temperature and inversely proportional to λ^3. If the DTS effect were significant, it would be seen in experiments to determine the Debye–Waller factor at various temperatures, and also in comparing the results of measurements at different setups.

After looking for simple reasons for the discrepancy between theory and experiment, Alexandrov and Ignatovich

hypothesized[34] that additional scattering is present which contributes to the Bragg peaks. This would arise from neutron scattering on regions of the tungsten sample which have ordered magnetic moments. This hypothesis was later confirmed experimentally in other experiments performed at the NPL in collaboration with the Leningrad Nuclear Physics Institute (Gatchina) and the Nuclear Physics Institute (Řež, Prague) [small-angle neutron scattering on ^{186}W samples with neutron depolarization,[35] neutron depolarization in diffraction on ^{186}W (Ref. 36)]. An activation analysis showed that the tungsten sample contains a tiny admixture of cobalt. Magnetic clusters containing a large number (hundreds) of tungsten atoms form around the cobalt atoms. Therefore, the NPL studies revealed the possible existence in tungsten of a heterophase state, i.e., a state simultaneously possessing the symmetry properties of two phases, the paramagnetic and the ferromagnetic. Although the study of heterophase states has now become an important area in physics (see, for example, Refs. 37–39), for the workers at NPL it represented a technical problem which took several years to solve. Similar effects have also been observed by other researchers,[40–42] for example, in palladium containing cobalt or iron impurities, in paramagnetic iron, and in several other compounds. We note that the presence of magnetic impurities is not essential for the formation of a heterophase state. The heterophase fluctuations existing in a very wide temperature range play an important role.[37,38]

Taking into account the formation of magnetic clusters, Eq. (42) takes a form describing combined nuclear and ferromagnetic scattering:[31,33]

$$I_{(hkl)}=C[(a+Zfa_{ne})^2+p^2]A_{(hkl)}\frac{\exp[-2B(\sin\theta/\lambda)^2]}{\sin 2\theta}, \tag{44}$$

where $p^2=\frac{2}{3}f_M^2a_M^2$, and f_M and a_M are the magnetic form factor and scattering length.

The NPL studies found the following value of a_{ne}, taking into account magnetic cluster formation:[31,35]

$$a_{ne}=(-1.60\pm0.05)\times10^{-3}\ \text{F}. \tag{45}$$

The dependence of the coherent scattering lengths for the two tungsten isotope mixtures obtained by including the p^2 term in (44) is shown in Fig. 3. Since even for ^{186}W the ratio $p^2/(a+Zfa_{ne})^2$ is only of order 10–20%, it is practically impossible to observe the effect of p^2 in experiments using naturally occurring tungsten.

The experiments discussed below to determine a_{ne} can be analyzed by two methods. Both are based on measurements of the energy dependence $\sigma_{\text{tot}}(E)$ at energies from 1 eV and higher, up to several keV, and, as a rule, on measurements of the neutron coherent scattering lengths at low energies (λ of the order of a few Å). To determine the value of a_{ne} by the first method, the energy dependence of σ_{tot} is analyzed, including all the unknown parameters: the nuclear radius, resonance scattering, the ne interaction, and so on. The same technique has been applied to the data of Refs. 43–45 and others. One of the most important and difficult-to-determine corrections in these experiments is that from resonance scattering. It is difficult to take this into account because there is no complete information about the resonance parameters, particularly for negative neutron energies.

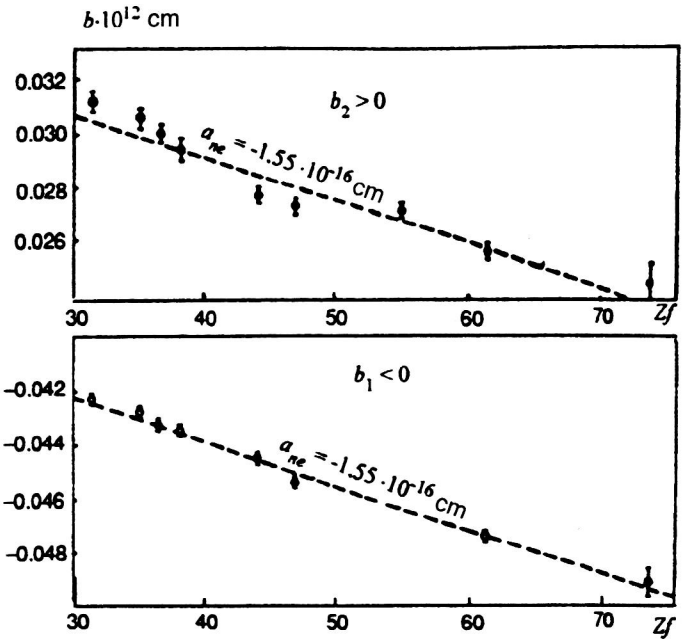

FIG. 3. Experimental dependence of the neutron coherent scattering lengths on Zf for two different isotope mixtures of tungsten, obtained after including the p^2 contribution.

The second method, which was developed and first applied at Dubna,[46] is to use an expression dealing with differences of measured quantities [see Eq. (53) below]. This expression does not involve the nuclear radius, and the effect of resonance scattering is considerably weaker than in the first method. As we shall show below, for even–even nuclei (for example, ^{208}Pb), resonance scattering has practically no effect on the results for a_{ne}.

In 1976–1995, in order to study ne scattering and also the electric polarizability of the neutron, Koester *et al.* (Garching, Germany) and collaborators at the JINR NPL (Refs. 43, 44, 47–49) measured the neutron coherent scattering lengths on lead, bismuth, and the isotope ^{208}Pb in a neutron gravity refractometer (see, for example, Ref. 10) and also by the method of small-angle neutron scattering using Christiansen filters. The resulting data were compared with the data on the neutron total cross sections on the same materials at neutron energies corresponding to resonances of rhodium (1.26 eV), silver (5.19 eV), tungsten (18.8 eV), and cobalt (132 eV). The measurements were performed using a continuously operating resonance detector composed of rotating disks made of resonance-absorber foil. The upper part of a disk was activated in the neutron beam, and the activity in the diametrically opposite part was recorded by β counters. This device ensured high statistical accuracy of the measurements. Measurements were later performed at two more energies: 1.97 and 143 keV. Neutrons of these energies were obtained by the technique of double resonance scattering and neutron beam filters (see, for example, Ref. 47). The results of measuring σ_{tot} for the neutron energy 143 keV are given in Ref. 50. In the same study it is pointed out that at this energy there is apparently an additional contribution

from resonance scattering which was neglected in analyzing the experimental results. In order to go from the total cross sections to the cross sections for elastic scattering and extrapolate them to thermal energies, it is necessary to introduce corrections into the measurement results for elastic incoherent scattering, effects related to the aggregate state of the matter, Schwinger scattering, and the energy dependence of the scattering due to resonances. Analysis of the results gave[43,44,47–49]

$$a_{ne}=(-1.32\pm0.03)\times10^{-3}\,\mathrm{F}. \tag{46}$$

However, in the opinion of the present author, the value (46) is not certain. The reason is that the energy dependence of the scattering from the contribution to the total cross section from unknown resonances and resonances with negative energy was taken into account by the Garching group in Ref. 44 and in part in the summary study[49] on the basis of knowledge of the average s-wave scattering parameters:[17] the strength function $s_0=\Gamma_n^0/D_0$, equal, for example, for bismuth, to 0.65 ± 0.15 (Ref. 17), and the average level spacing $\langle D_0\rangle=4.5\pm0.6$ keV (also for bismuth[17]). It is easy to make an error here, because a resonance (or several resonances) at $E_{0j}<0$, for example, can lie at a distance $|E_{0j}|<\langle D_0\rangle$ from the point $E=0$. Moreover, the errors in the known values of s_0 and $\langle D_0\rangle$ are quite large (up to 23% for bismuth).

The result found at the NPL in 1985 appears more realistic. It was obtained by measuring the total cross section for bismuth by the time-of-flight method in the energy range 1–130 eV using the beam of the IBR-30 pulsed reactor.[46] The possibility of a combined description of nuclear and ne scattering and scattering due to the electric polarizability of the neutron at these energies was also considered in the NPL studies (Refs. 10, 46, 51, and 52). The formalism[16] often applied to the problem of particle scattering on a sum of short- and long-range potentials was used. The total amplitude f_t for neutron scattering on an atom can be expressed in terms of the phase shifts for nuclear scattering δ_l, ne scattering η_l, and polarization scattering ε_l:

$$f_t=\frac{1}{2ik}\sum_l (2l+1)\{S_l\exp[2i(\eta_l+\varepsilon_l)]-1\}P_l(\cos\varphi), \tag{47}$$

where S_l is the nuclear scattering matrix, $\Delta E_i=E-E_i$, E_i is the energy of the ith resonance, and Γ_{ni} and Γ_i are the neutron and total width of the ith resonance. As a first approximation, we can take the nuclear scattering matrix to be the usual one:

$$S_l=\left(1-\sum_i \frac{i\Gamma_{ni}}{\Delta E_i+i\Gamma_i/2}\right)\exp(2i\delta_l). \tag{48}$$

At low energies, when only s-wave scattering is important for the nucleus, (47) can be reduced to the form

$$f_t=\frac{1}{2ik}(S_0-1)\exp[2i(\eta_0+\varepsilon_0)]+\frac{1}{k}\sum_l (2l+1)\sin(\eta_l+\varepsilon_l)\exp[i(\eta_l+\varepsilon_l)]P_l(\cos\varphi). \tag{49}$$

Let us first consider the case of potential scattering (neglecting resonances). Using the first Born approximation to determine the ne and polarization scattering, we find

$$f_t=\frac{1}{2ik}[\exp(2i\delta_0)-1]\exp[2i(\varepsilon_0+\eta_0)]+f_n(\varphi)+Zf(\sin\varphi/\lambda)a_{ne}, \tag{50}$$

where $f(\sin\varphi/\lambda)$ is the atomic form factor, $\varepsilon_0=M\alpha_n(Ze/\hbar)^2(k/R-\pi k^2/3)+\ldots$ (Ref. 10) is the phase shift of the polarization scattering, α_n is the electric polarizability of the neutron, and $\eta_0=\frac{1}{2}ka_{ne}\int_0^\pi f(\sin\varphi/\lambda)\sin\varphi d\varphi$ (Ref. 10) is the phase shift of ne scattering. It follows from (50) that

$$\mathrm{Re}\,f_t=\sin\delta_0\cos[\delta_0+2(\eta_0+\varepsilon_0)]/k+f_n(\varphi)+Zf(\sin\varphi/\lambda)a_{ne}=-b_{\mathrm{coh}}A/(A+1), \tag{51}$$

$$\mathrm{Im}\,f_t(0)=\sin\delta_0\sin[\delta_0+2(\eta_0+\varepsilon_0)]/k=k\sigma_{\mathrm{tot}}/(4\pi). \tag{52}$$

These expressions contain the unknown quantities δ_0, a_{ne}, and α_n, which can be found by substituting into (51) and (52) the experimental values of b_{coh} and σ_{tot} obtained at several energies.

Taking into account resonances, Eqs. (51) and (52) become

$$\mathrm{Re}\,f_t=\frac{1}{k}\left\{\sin\delta_0\cos[\delta_0+2(\eta_0+\varepsilon_0)]-\frac{1}{2}\cos 2(\delta_0+\eta_0+\varepsilon_0)\sum_i\frac{g\Gamma_{ni}\Delta E_i}{(\Delta E_i^2+\Gamma_i^2/4)}-\frac{1}{2}\sin 2(\delta_0+\eta_0+\varepsilon_0)\sum_i\frac{\Gamma_{ni}\Gamma_i/2}{(\Delta E_i^2+\Gamma_i^2/4)}\right\}\approx\delta_0/k-\frac{1}{2k}\sum_i\frac{g\Gamma_{ni}\Delta E_i}{(\Delta E_i^2+\Gamma_i^2/4)}, \tag{51'}$$

$$\mathrm{Im}\,f_t(0)/k=\sigma_{\mathrm{tot}}/4\pi=\frac{1}{k^2}\left\{\sin\delta_0\sin[\delta_0+2(\eta_0+\varepsilon_0)]-\frac{1}{2}\sin 2(\delta_0+\eta_0+\varepsilon_0)\sum_i\frac{g\Gamma_{ni}\Delta E_i}{(\Delta E_i^2+\Gamma_i^2/4)}+\frac{1}{4}\cos 2(\eta_0+\varepsilon_0)\sum_i\frac{g\Gamma_n^2}{(\Delta E_i^2+\Gamma_i^2/4)}+\frac{1}{4}\cos 2(\eta_0+\varepsilon_0)\sum_i\frac{g\Gamma_{ni}\Gamma_\gamma}{(\Delta E_i^2+\Gamma_i^2/4)}\right\}. \tag{52'}$$

From these we find the expression used to analyze the experimental data obtained in Ref. 46:

$$y=\sigma_{\mathrm{tot}}(E')/4\pi-b^2{}_{\mathrm{coh}}A/(A+1)=a^2{}_{ne}(Z-F)^2-2a_{ne}b_{\mathrm{coh}}A(Z-F)/(A+1)-f^2+2a_{ne}fF+2/3\pi k'Rfb_{\mathrm{coh}}A/(A+1)-(\Sigma_1-\Sigma)[b_{\mathrm{coh}}A/(A+1)+a_{ne}(Z-F)+\pi k'Rf/3]+(\Sigma_1)^2/4-\Sigma_1\Sigma/2+\Sigma_2/4$$

$$+\sigma_{abs}(E')/(4\pi), \tag{53}$$

where $f=(M\alpha_n/R)(Ze/\hbar)^2$ is the scattering amplitude due to the electric polarizability of the neutron; $F=(Z/2)\int_0^\pi f(\sin\theta/\lambda)\sin\theta d\theta$ is the atomic form factor integrated over angles; E and E' are the neutron energies at which b_{coh} and σ_{tot} are measured; $\sigma_{abs}(E')=(\pi/k'^2)\Sigma_i[g_i\Gamma'_{ni}\Gamma_{\gamma i}/(\Delta E_i'^2+\frac{1}{4}\Gamma_i'^2)]$ is the absorption cross section; E_i, Γ_{ni}, and $\Gamma_{\gamma i}$ are the energy and the neutron and γ widths of the ith resonance;

$$\Sigma_1=\Sigma_i[g_i\Gamma_{ni}\Delta E_i/k(\Delta E_i^2+\tfrac{1}{4}\Gamma_i^2)],$$
$$\Sigma=\Sigma_i[g_i\Gamma'_{ni}\Delta E'_i/k'(\Delta E_i'^2+\tfrac{1}{4}\Gamma_i'^2)], \tag{54}$$
$$\Sigma_2=\Sigma_i[g_i\Gamma_{ni}'^2/k'^2(\Delta E_i'^2+\tfrac{1}{4}\Gamma_i'^2)].$$

The value $y\approx 0.015-0.020$ b/sr was found for bismuth.

For $E\ll E_i$ and $\Gamma_i\ll\Delta E_i$ the terms containing resonances can be written as expansions in E/E_i, and we find[46]

$$p_1=E'\frac{k'\sigma_{abs}(E')}{\pi\langle\Gamma_\gamma\rangle} \tag{55}$$

and

$$p_2=\frac{1}{4}\sum_i\frac{g_1\Gamma_{ni}^2}{k_i^2E_i^2}-\frac{1}{4}\left(\sum_i\frac{g_i\Gamma_{ni}}{k_iE_i}\right)^2 \tag{56}$$

(neglecting the inter-resonance interference contribution $\Delta\sigma_{int}/4\pi$).

The contribution to y from the p_1 term can be determined by substituting the numerical values of $\sigma_{abs}(E)$ and $\langle\Gamma_\gamma\rangle$ from the literature (see, for example, Ref. 17) into (55). Then, for example, for bismuth, we have the product $p_1b_{coh}=5.12\times10^{-4}$ b/sr at a neutron energy of 10 eV. The contribution to y from the p_2 term, which includes the resonance contribution and also inter-resonance interference, is estimated to be a few percent for bismuth. However, it cannot be determined exactly, owing to the lack of information about levels with negative energy. Its value should be varied, as was done in Ref. 46, and then chosen so as to obtain the best description of the experimental data (see below for the analytic determination of $p_2+\Delta\sigma_{int}/4\pi$).

The measurements of Ref. 46 were performed using a 60-meter flight path with both melted and solid samples of bismuth of thickness 18 mm. The background level measured by placing rhodium, silver, and tungsten disks in the beam (resonance energies 1.26, 5.19, and 18.83 eV) was low (0.3–0.4% at energies 1–6 eV and less than 1.5% at around 20 eV). The detector was a counter filled with ^{3}He gas at a pressure of 8 atm. The correction for the dead time was found by passing the neutrons through lead plates of various thicknesses. It was less than 1.5%. The distance between the detector and the sample (about 2 m) excluded the possibility of any effect of small-angle neutron scattering on the energy behavior of σ_{tot} (see below for a discussion of this effect). The energy dependence of the total cross section for neutrons interacting with bismuth obtained in Ref. 46 is shown in Fig. 4. First, the experimental data for energies from 1 to 20 eV were corrected for Schwinger scattering and the aggregate state of the sample. For bismuth these corrections were less

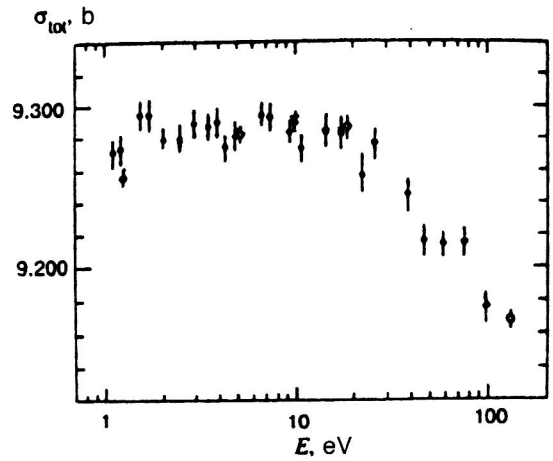

FIG. 4. Dependence of σ_{tot} (b) on the neutron energy E (eV): ● are the NPL data,[46] and ○ and × are the Garching data.[43,44,53]

than 0.8% of the total cross section. In the same figure we give the values of $\sigma_{tot}(E)$ measured at the Garching laboratory (Munich).[43,44,53] They were used to determine the absolute values of σ_{tot} found in Ref. 46. The inter-resonance interference term was found using the corresponding scattering matrices (see below). For the known resonances of bismuth it was $\Delta\sigma_{int}=0.108\times10^{-24}$ cm^2 at neutron energy 10 eV, which is about 90 times smaller than the total cross section for bismuth. In the case of bismuth, at energies below 50 eV it can be considered practically independent of the neutron energy. Therefore, the addition to the p_2 term [see Eq. (56)] of the extra contribution $\Delta\sigma_{int}$ cannot change the result for a_{ne} found in Ref. 46, although, of course, it does change the analytic expression for p_2. In Ref. 46 the p_2 term was assumed to be unknown and was varied to obtain the best description of the experimental data by (53). The experimental data were analyzed by the least-squares method. The value of the p_2 term was found to be -0.0023 b/sr. The data of the Garching group[43,44,53] were analyzed separately using this value of p_2. The results are given in Table I.

Therefore, the analysis of the Garching results using the value of p_2 found in Ref. 46 increases the absolute value of a_{ne} given in Table I by about a factor of 1.2 and gives $\langle r_{E,in}^2\rangle_N<0$. The data obtained on a_{ne} agree with those of the Dubna diffraction measurements[31] performed using single crystals of tungsten.

Yet another result for the neutron–electron scattering length was obtained in 1994–1995 at the JINR NPL.[54] The total neutron cross section was measured for a lead sample containing 98.3% of the isotope ^{208}Pb and of purity 99.98%. The sample was a metal cylinder of diameter 15 mm and thickness 20.8 mm. The diameter of the neutron beam was 11 mm at the sample surface. The measurements were per-

TABLE I.

	Garching data[43,44,53]	Dubna data[46]
a_{ne}	$(-1.57\pm0.10)\times10^{-3}$ F	$(-1.55\pm0.11)\times10^{-3}$ F

formed on the 70-meter flight path of the IBR-30 booster using the time-of-flight method. The neutron detector was a cylinder of length 20 cm filled with ^{3}He gas at a pressure of 10 atm. The detector was located 1 m from the sample, and thus the possible effect of small-angle scattering on the energy behavior of the lead cross section was eliminated for neutron energies ranging from 1 eV to 24 keV (see below). The background in the measured total cross section for lead at a neutron energy of 100 eV was determined using "black" Cd, Ag, W, and Co filters. The second neutron energy range from 3 to 8 keV was isolated using not only the time-of-flight method, but also a 4-cm filter of Na_2CO_3 (^{23}Na has a resonance at 2.85 keV) and a 10-cm filter of ^{60}Ni with cross section strongly varying from 0.01 to 200 b for neutron energies in the range from 4 to 12 keV. Finally, the third range near 24 keV was separated by using, in addition, filters of iron (24 cm) and aluminum (10 or 20 cm).

One of the essential corrections introduced by the authors in determining the absolute value of $\sigma_{\rm tot}$ was the correction for the dead time of the electronics (including the detector). The error in $\sigma_{\rm tot}$ when this correction was introduced reached a value $\Delta\sigma_{\rm tot}\approx\pm 7$ mb. However, since a_{ne} depends mainly on the energy behavior of the curve $\sigma_{\rm tot}(E)$, the value of $\Delta\sigma_{\rm tot}$ from introducing the correction for the dead time cannot strongly affect the value found for a_{ne}. The scattering cross section σ_{sc} was obtained from $\sigma_{\rm tot}$ after subtracting the capture cross section, the contribution of solid-state effects, and the cross section for Schwinger scattering. Finally, the cross section for neutron potential scattering by lead-208, $\sigma_{\rm pot}^{208}$, was determined from $\sigma_{\rm sc}$. The contribution of the other isotopes and s-wave resonance effects of the ^{208}Pb nuclide was included.

Taking $\sigma_{\rm pot}^{208}=(4\pi/k^2)\sin^2\delta_0$, where $\delta_0=-k(R+a_{ne}ZF+a_{\rm p}Q)$ is the total scattering phase shift, $R'=R_0'-hE$, h includes the contribution of unknown resonances of ^{208}Pb, $a_{\rm p}$ is the scattering amplitude due to the electric polarizability of the neutron, $Q=1-(5\pi/18)kR_N+\ldots$, and F is the atomic form factor integrated over angles, the parameters R_0', h, a_{ne}, and $a_{\rm p}$ were fit. The resulting value of a_{ne} was

$$a_{ne}=(-1.67\pm 0.16)\times 10^{-3}\,\mathrm{F}, \tag{57}$$

with a value of χ^2 roughly half that for $a_{ne}=-1.32\times 10^{-3}$ F. However, the NPL measurements[54] did not achieve good enough accuracy to permit definite conclusions about a_{ne} to be drawn.

Among the recent experiments, mention should be made of the joint Austrian–American studies carried out in 1992–1995 at Oak Ridge using the pulsed neutron source ORELA.[45] The experiments were largely based on the approach taken in earlier measurements.[20] However, a number of important improvements were made. They are the following. The use of the time-of-flight method allowed a considerably more accurate determination of the neutron energy than in Ref. 20, where a crystal spectrometer was used (energies 0.1, 0.28, 1.0, and 4 eV). The admixture of neutrons of other energies from higher reflection orders present in Ref. 20 was thus eliminated. When performing measurements using the time-of-flight method there was no need to change the experimental geometry. It remained the same for all incident neutron beam energies, whereas in Ref. 20 it was necessary to change the scattering angle of the crystal spectrometer. Owing to the increased sample thickness, the sensitivity of the later study to the measured ne effect was higher than in the earlier experiment:[20] the change of the sample transmission due to the ne interaction was $\approx 3\%$ as the neutron energy varied from 0.1 to 2 eV (in Ref. 20 it was about 1.4%).

The detector was lithium glass and was located 18.8 m from the neutron source. The distance from the source to the sample and the resonance filters for determining the background was 5, 9, and 10 m. For neutron energies in the range from 0.1 to 100 eV the ratio of the number of useful counts to the background reached 1500. The dead time of the system was less than 0.5% for the neutron beam without the sample, and about 0.1% with the sample.

The transmission of the neutron beam through the sample is

$$T(E)=\exp[-\sigma_{\rm tot}(E)N], \tag{58}$$

where $N=0.154$ atoms/b is the thickness of the studied sample. The total neutron cross section is

$$\sigma_{\rm tot}(E)=\sigma_{\rm coh}(E)S_{\rm coh}(E)+\sigma_{\rm inc}(E)S_{\rm inc}(E)+\sigma_{\rm abs}(E), \tag{59}$$

where $S_{\rm coh}(E)$ and $S_{\rm inc}(E)$ are functions describing the corrections due to the aggregate state of the sample.

The isotope content of the lead sample was 72.54% ^{208}Pb, 1.65% ^{207}Pb, 25.82% ^{206}Pb, and 0.5% ^{204}Pb, which ensured a very small neutron-capture cross section $\sigma_{\rm abs}$ (of order 3 mb at 1 eV). The sample was in the liquid state at a temperature of about 625 K.

The cross section for coherent scattering in the first Born approximation is

$$\sigma_{\rm coh}(E)=4\pi\{a_{\rm coh}(E)+a_R(E)-a_{ne}Z[1-f(\sin\theta/\lambda)]+a_p(E)\}^2+\sigma_{\rm Sch}(E), \tag{60}$$

where $a_{\rm coh}(E)$ is the nuclear coherent scattering length, $a_{\rm R}(E)$ is the nuclear resonance scattering length, $a_{\rm p}(E)$ is the scattering length due to the electric polarizability of the neutron, and $\sigma_{\rm Sch}(E)$ is the cross section for Schwinger scattering.

The transmission data were analyzed by the least-squares method. The value of a_{ne} and the normalization parameter (the nuclear coherent scattering length of bismuth) were varied in the energy range from 0.1 to 360 eV. The value found was

$$a_{ne}=(-1.31\pm 0.03\pm 0.04)\times 10^{-3}\,\mathrm{F}, \tag{61}$$

which according to (16) and (20) gives

$$\langle r_E^2\rangle=-0.113\pm 0.003\pm 0.004\,\mathrm{F}^2 \tag{62}$$

or $\langle r_{E,\rm in}^2\rangle>0$ [according to (19)]. The first error in (61) and (62) is statistical, and the second is systematic. About 75% of it is due to the uncertainties in calculating the corrections due to the aggregate state of the matter. The remaining 25%

TABLE II.

Authors, year	Method	Target	Magnitude of effect	$-a_{ne}[10^{-3}$ F]	Reference
Havens *et al.*, 1947–51	Energy dependence of the total cross section	Lead and bismuth	$\Delta\sigma_{ne}/\sigma_{tot}\approx 1.5\%$	1.91 ± 0.36	18
Hughes *et al.*, 1952–53	Neutron reflection	O_2-Bi mirror	$\Delta\theta/\theta\approx 50\%$	1.39 ± 0.13	25
Melkonian *et al.*, 1959	Energy dependence of the total cross section	Bismuth	$\Delta\sigma_{ne}/\sigma_{tot}\approx 1.5\%$	1.56 ± 0.05	20
Krohn and Ringo, 1966–73	Scattering asymmetry	Noble gases	$\Delta\sigma_{ne}/\sigma_{tot}\approx 0.5\%$	1.33 ± 0.03	15
Koester *et al.*, 1976–95	Energy dependence of the total cross section and measurement of the scattering length	Bismuth, lead, and lead-208	$\Delta\sigma_{ne}/\sigma_{tot}\approx 1.2\%$	1.32 ± 0.03	43,44, 47,49
Aleksandrov *et al.*, 1985	Energy dependence of the total cross section	Bismuth	$\Delta\sigma_{ne}/\sigma_{tot}\approx 1.2\%$	1.55 ± 0.11	46
Kopecky *et al.*, 1994–95	Energy dependence of the total cross section	Lead (72.5% ^{208}Pb)	$\Delta\sigma_{ne}/\sigma_{tot}\approx 1.2\%$	$1.31\pm 0.03\pm$ 0.04	45,63
Enik *et al.*, 1995	Energy dependence of the total cross section	Lead-208	$\Delta\sigma_{ne}/\sigma_{tot}\approx 1.2\%$	1.67 ± 0.16	54
Aleksandrov *et al.*, 1974–85	Neutron diffraction	Tungsten-186 single crystal	$\Delta\sigma_{ne}/\sigma_{tot}\approx 20\%$	1.60 ± 0.05	31,35

of the error is due to uncertainties in determining the background, the contribution of resonance scattering, and the dead time of the system.

It should be noted that since the correction functions $S_{coh}(E)$ and $S_{inc}(E)$ grow strongly with decreasing neutron energy, the transmission data were fit for various energy ranges independently. It is also noteworthy that the value of a_{ne} depends only on the energy dependence of $\sigma_{tot}(E)$, and not on its absolute value.

The results of measurements of the ne scattering length performed from 1947 to 1995 are given in Table II. We see from this table that to find $a_{ne}-a_F=(Me^2/3\hbar^2)\langle r^2_{E,in}\rangle_N$, i.e., to measure the neutron intrinsic charge radius $\langle r^2_{E,in}\rangle^{1/2}_N$, the accuracy of the measurements must be increased. The only thing that can now be said about $\langle r^2_{E,in}\rangle^{1/2}_N$ is that it is small, apparently less than 0.1 F.

It should be noted that if $\langle r^2_{E,in}\rangle^{1/2}_N$ for the neutron were the same as for the proton (0.83 F), then a_{ne} would be of order 10^{-2} F, i.e., roughly 6–8 times larger than the values given in Table II.

It also follows from Table II that there are two groups of experimental results: $\langle a_{ne}\rangle=-1.30(3)\times 10^{-3}$ F ($\langle r^2_{E,in}\rangle_N>0$) and $\langle a_{ne}\rangle=-1.58(3)\times 10^{-3}$ F ($\langle r^2_{E,in}\rangle_N<0$). Making these two groups of results consistent and understanding the reasons for the discrepancy is very important for the theory.[10,55]

5. CORRECTIONS INTRODUCED INTO THE EXPERIMENTS. SOURCES OF POSSIBLE SYSTEMATIC ERROR

The determination of the scattering length a_{ne} is based on precision measurements of the total neutron cross sections and scattering lengths ($\Delta\sigma_{tot}/\sigma_{tot}=\Delta a/a\approx 10^{-3}-10^{-4}$). To achieve such accuracy it is necessary to introduce a number of corrections. In addition, difficulties arise in finding and eliminating possible sources of systematic error (see, for example, Ref. 56).

First, it is necessary to have reliable methods of determining the background. As a rule, the background should not exceed 1–2% of the measured useful intensity. It should not vary strongly when experimental parameters (such as the neutron energy or the scattering angle) are changed.

Second, in measuring the total cross sections it is necessary to minimize the correction for detector counting errors at large counting rates. As a rule, the dead time of the detector and the electronics circuit should be no more than 0.5 μsec.

Third, special attention should be paid to effects which directly distort the measured quantities. For example, in measuring total cross sections on long flight paths (for example, in Ref. 45) at small solid angle of the detector, the energy behavior of the cross section can be distorted by

small-angle neutron scattering on the sample. For sufficiently large solid angle, small-angle neutron scattering always lies inside the detector area and has no effect on measurement of the transmission at various energies, although small-angle scattering varies strongly with the neutron energy. Small-angle scattering encompasses the range of scattering angles from one angular second to several degrees as the neutron wavelength varies from 1 to 20 Å. An expression for the differential cross section of small-angle neutron scattering can be found in a number of published studies, in particular, Refs. 57 and 58. For spherical inhomogeneities of radius R in the sample (usually $R \approx 20-40$ Å), it has the form

$$\sigma_{sa}(\theta) = Na^2 \exp(\varkappa^2 R^2/5), \tag{63}$$

where $\kappa = 2k \sin(\theta/2) \approx k\theta$, a is the scattering length, and N is the number of scattering atoms in each inhomogeneity. Small-angle neutron scattering occurs on individual inhomogeneities and leads to the appearance of an additional component of the neutron beam scattered by the sample. The cross section $\sigma_{sa}(0)$ at $\theta = 0$, i.e., the forward cross section, can be large, but it falls off rapidly with increasing scattering angle.

The principles underlying small-angle scattering are diverse (clusters of structural defects, magnetic heterophase fluctuations, etc.). Heterophase fluctuations can have a dynamical nature, i.e., their number and size can vary with time. Their microscopic description is being studied by a group of theoreticians at the JINR (see, for example, Refs. 37 and 38).

A large number of setups have been built all over the world for the experimental study of small-angle neutron scattering. One of them is at the Petersburg Nuclear Physics Institute in Gatchina. Small-angle neutron scattering by a tungsten-186 sample has been studied there.[35] As a rule, small-angle neutron scattering occurs on almost all solid materials. At the PNPI setup it was even found on cadmium (at $\lambda \approx 8.8$ Å; see Ref. 35).

Systematic errors can also arise when the experimental data are not analyzed completely correctly, in particular, when resonance nuclear scattering is included. When analyzing data on total cross sections it is necessary to include the effect of resonances located far from the energy range studied. Whereas for levels with positive energy this procedure can in principle be performed for all the known resonances, for levels with negative energy it is impossible, owing to the lack of information about such levels. Such inaccuracies in analyzing the experimental data have been tolerated in, for example, Refs. 44 and 49.

In several studies (see, for example, Ref. 54) the effect of resonances located far from the studied energy range (including ones at negative neutron energies) was taken into account by adding an extra term hE to the scattering range, where h is a parameter obtained by expanding the first resonance term in Eq. (52′) in a series in E/E_i:

$$h = -2276(A+1)/(A)\Sigma g\Gamma_n^0/E_i^2 \text{ F/eV}. \tag{64}$$

The parameter h can also be estimated by measuring the energy dependence of σ_{tot} in a wide energy range. Such a study was performed for ^{208}Pb in Ref. 59. Here it is also important to note that in analyzing the difference $y = \sigma_{tot}/4\pi - b_{coh}^2$ for even–even nuclei (for example, ^{208}Pb), resonance scattering has practically no effect on the results for a_{ne} (see Sec. 6 below).

TABLE III.

Temperature, °K	603	623	673	763
$C(T)$, 10^{-3} eV	0.963	0.952	0.935	0.931
$l\lambda^2/(8\pi V_0^{2/3})E$, 10^{-3} eV	0.966	0.966	0.966	0.966

Fourth, for energies in the eV range it is necessary to include corrections both for interference with nuclei adjacent to the studied nucleus embedded in the crystal lattice, and for the thermal motion of the atoms (the Doppler effect). These corrections have been studied in Refs. 60–62. Both of them decrease with increasing neutron energy, and already for $E \geqslant 1$ eV it is possible to use an interference term of the form[60]

$$\Delta\sigma/\sigma = l\lambda^2/(8\pi V_0^{2/3}), \tag{65}$$

where l is a coefficient equal to 2.885 for liquid lead and bismuth, and V_0 is the atomic volume. The Doppler correction is given by[61]

$$\sigma/\sigma_{free} = 1 + \frac{k_B T}{2E} \cdot \frac{m}{M}, \tag{66}$$

where m is the nucleon mass, M is the atomic mass, k_B is the Boltzmann constant, and T is the sample temperature in degrees Kelvin.

Similar expressions can also be obtained from the data of Ref. 63, which give

$$S_{coh}(E) = 1 + \frac{k_B T}{2E} \cdot \frac{m}{M} - \frac{C(T)}{E} \tag{67}$$

and

$$S_{inc}(E) = 1 + \frac{k_B T}{2E} \cdot \frac{m}{M}. \tag{68}$$

The value of $C(T)$ depends both on the sample material and on its temperature. It was determined in Ref. 63 for neutron energies in the range 0.001–500 eV for liquid lead. The results are given in Table III. The error in determining $C(T)$ is less than 5%.

Fifth, a correction must be introduced into the experimental data for Schwinger scattering, due to the interaction of the moving magnetic moment of the neutron with the Coulomb field of the nucleus. The amplitude of Schwinger scattering has the form[10]

$$f_{Sch}(\varphi) = \frac{i}{2}(\boldsymbol{\sigma}\mathbf{n})\mu_n\left(\frac{\hbar}{Mc}\right)\left(\frac{Ze^2}{\hbar c}\right)[1 - f(q)]\cot\frac{\varphi}{2}, \tag{69}$$

where $f(q) = (4\pi/Z)\int_0^\infty (\sin qr/qr)\rho(r)r^2 dr$ is the atomic form factor, well known from the theory of x-ray scattering by atoms, $q = 2k \sin(\varphi/2)$, $e\rho(r)$ is the electric charge density at the point r, $\boldsymbol{\sigma}$ is the spin matrix, and $\mathbf{n}$ is related to $\mathbf{k}$ and $\mathbf{k}_0$ as $[\mathbf{k} \times \mathbf{k}_0] = \mathbf{n}k^2 \sin\varphi$, where, in turn, $\mathbf{k}$ and $\mathbf{k}_0$ are the final and initial wave vectors of the scattering.

TABLE IV. Corrections to the measured total cross sections (in barn).

Energy, eV	S_{coh}	$\Delta\sigma=\sigma_{exp}(1-S_{coh})$ ($\sigma_{exp}=11$ b)	Schwinger scattering (σ_{Sch}, b)
1.26	0.9993436	0.0072	0.0029
5.19	0.9998407	0.0018	0.0046
10.1	0.9999181	0.0009	0.0055

When measuring transmission, Schwinger scattering must be included, using the expression

$$\sigma_{Sch}=\frac{\pi}{2}\mu_n^2\left(\frac{\hbar}{Mc}\right)^2\left(\frac{Ze^2}{\hbar c}\right)^2 \times\int_{\varphi_0}^{\pi}[1-f(q)]^2\cot^2\frac{\varphi}{2}\sin\varphi d\varphi, \quad (70)$$

where the scattering angle φ_0 is chosen according to the experimental geometry.

An example of the numerical values of the corrections introduced into σ_{tot} for lead-208 as a function of the neutron energy is given in Table IV.

Sixth, care should be taken in introducing corrections for the effect of p-wave scattering into the cross section. Estimates show that the cross section for p-wave scattering ($\sigma_1=(4\pi/k^2)3\sin^2\delta_1$) makes up about 0.5% of the s-wave cross section ($\sigma=(4\pi/k^2)\sin^2\delta_0$) at a neutron energy of about 20 keV. To take into account p-wave scattering it is necessary to determine the phase δ_1. In the case of neutrons we can use the relations published in Ref. 64:

$$\exp(2i\delta_l)=\frac{G_l(R)-iF_l(R)}{G_l(R)+iF_l(R)}, \quad (71)$$

where R is the channel radius, $G_l(R)=-\sqrt{\frac{1}{2}\pi kR}N_{l+1/2}(kR)$, and $F_l(R)=-\sqrt{\frac{1}{2}\pi kR}J_{l+1/2}(kR)$. At low energies ($kR\ll 1$), from (71) we find the well known limiting expression:

$$\delta_1\approx\frac{-(kR)^{2l+1}}{(2l-1)!!(2l+1)!!} \quad (72)$$

or $\delta_1=-(kR)^3/3$. The calculations of Guseva[65] (PNPI, Gatchina) showed that the difference between the values of σ_1 when (71) and (72) are used is 10% at $E=24$ keV, 25% at $E=45$ keV, and 40% at $E=145$ keV. This implies that (71) should be used for estimates. As far as experiment is concerned, it is necessary to find, if possible, experimental methods of determining p-wave scattering, as was done, for example, in Ref. 66.

Finally, seventh, we note that in a number of studies (for example, Refs. 67 and 68) used to analyze measurement results, the fit of the expansion of the total cross section for potential scattering in powers of the wave vector k

$$\sigma_{sc}(k)=\sigma_{sc}(0)+ak+bk^2+ck^3+dk^4+\ldots \quad (73)$$

does not contain the term proportional to k^3. However, (73) can be obtained from a series expansion of the expression describing the cross section for potential scattering, $\sigma_{sc}=(4\pi/k^2)\sin\delta_0\sin(\delta_0+2\eta_0)$ [see (52)]. Here the k^3 term must be present in (73). The ratio of this term to the term proportional to the wave vector k is $\frac{2}{3}(kR)^2$ and equal to 7% at 20 keV, 10% at 40 keV, and 20% at 145 keV. Therefore, the term proportional to k^3 must be included in analyzing the experimental data. This is especially important when performing measurements at relatively high energies (the keV range), for example, in the attempts to measure the neutron electric polarizability.[67,68] It should also be noted that writing the neutron scattering cross section in powers of the wave number is suitable only at energies where $\sin\delta_0\approx\delta_0$, i.e., no more than a few keV. Otherwise, the fact that the phase shift occurs inside the argument of the sin function must be taken into account.

6. THE INCLUSION OF INTER-RESONANCE INTERFERENCE

The absence of inter-resonance interference terms in the expression for the scattering cross section is a consequence of the particular form of the components of the S matrix, where the contributions of individual resonances to the scattering matrix add. This description is an approximation. However, S matrices including inter-resonance interference in neutron scattering on nuclei have been known for quite a long time (see, for example, Refs. 69–71). One of them has the form[71]

$$S_{nn}=\left(1-i\sum_j\frac{\alpha_{nj}+i\beta_{nj}}{E-\mu_j+i\nu_j}\right)\exp(2i\delta_{pot}), \quad (74)$$

where $\Sigma(\alpha_{nj}+i\beta_{nj})=\Sigma\Gamma_{nj}$, $\Sigma\beta_{nj}=0$, $\mu_j=\mathrm{Re}\,\tilde{E}_j$, $\nu_j=\mathrm{Im}\,\tilde{E}_j$, and $\tilde{E}_j$ is the complex energy of the jth resonance (for $\beta_{nj}=0$, $\tilde{E}_j=E_j+(i/2)\Gamma_j$). For $\beta_{nj}=0$, σ_{tot} is the sum of Breit–Wigner terms including only the interference between potential and resonance scattering. When all the resonance levels of (74) are included, the calculation of σ_{tot} using

$$\sigma_{tot}=2\pi g(1-\mathrm{Re}\,S_{nn})/k^2 \quad (75)$$

is quite complicated. In Ref. 72, Eqs. (74) and (75) were used to obtain a two-level expression for σ_{tot} which qualitatively interprets all the main features of the correlations between the values of the resonance parameters of the levels. It has the form

$$\sigma_{tot}=\sigma_{pot}+\frac{2\pi g}{k^2}\left[\frac{G_1\nu_1+H_1(\mu_1-E)}{(\mu_1-E)^2+\nu_1^2}+\frac{G_2\nu_2+H_2(\mu_2-E)}{(\mu_2-E)^2+\nu_2^2}\right], \quad (76)$$

where

$$G_1=\alpha_{1n}\cos 2\delta_{pot}+\beta_n\sin 2\delta_{pot},$$

$$G_2=\alpha_{2n}\cos 2\delta_{pot}-\beta_n\sin 2\delta_{pot},$$

$$H_1=\beta_n\cos 2\delta_{pot}-\alpha_{1n}\sin 2\delta_{pot},$$

$$H_2=-\beta_n\cos 2\delta_{pot}-\alpha_{2n}\sin 2\delta_{pot},$$

$$\alpha_{1n}+iB_{1n}=\tilde{\Gamma}_{1n},\quad \alpha_{2n}-i\beta_{2n}=\tilde{\Gamma}_{2n},$$

TABLE V.

	Bismuth ($E_1=800$ keV, $E_2=2310$ keV)			Lead-208 ($E_1=507$ keV, $E_2=1735$ keV)	
Energy, eV	1	16	50	1000	25000
$\Delta\sigma_{\text{int}}$, 10^{-3} b	±20.7	±20.0	±20.5	±4.9	±4.2

$$2\tilde{E}_{1,2}=\bar{E}_1-i\Gamma_1/2+E_2-i\Gamma_2/2\mp[(E_2-i\Gamma_2/2-E_1+i\Gamma_1/2)^2-\Gamma^2_{12}]^{1/2},$$

$$\tilde{\Gamma}_{1n}=\Gamma_{1n}\cos^2\varphi+\Gamma_{2n}\sin^2\varphi+\Gamma^{1/2}_{1n}\Gamma^{1/2}_{2n}\sin 2\varphi,$$

$$\tilde{\Gamma}_{2n}=\Gamma_{2n}\cos^2\varphi+\Gamma_{1n}\sin^2\varphi-\Gamma^{1/2}_{1n}\Gamma^{1/2}_{2n}\sin 2\varphi,$$

$$B=i\Gamma_{12}[(E_2-E_1-i\Gamma_2/2+i\Gamma_1/2)^2-\Gamma^2_{12}]^{1/2},$$

$\varphi=\sin^{-1}(B/2)$ and $\Gamma_{12}=(\Gamma_1\Gamma_2)^{1/2}$; in our case, $\Gamma^2_{12}\ll(E_2-E_1)^2$. The results of calculating the inter-resonance interference terms $\Delta\sigma_{\text{int}}$ using (75) for bismuth (resonance energies $E_1=800$ eV and $E_2=2310$ eV) and ^{208}Pb (resonance energies $E_1=507$ keV and $E_2=1735$ keV) are given in Table V.

The signs of $\Delta\sigma_{\text{int}}$ are determined by the choice of sign of the square roots of $\tilde{\Gamma}_{1n}$, $\tilde{\Gamma}_{2n}$, B, and Γ_{12}. It follows from Table V that far from the resonance energies the values of $\Delta\sigma_{\text{int}}$ are practically independent of energy and amount to only a fraction of a percent of σ_{tot} (0.2% of σ_{tot} for bismuth and 0.04% of σ_{tot} for ^{208}Pb).

Another expression for the S matrix can be taken, for example, from Refs. 69 and 70:

$$S_{cc'}=\exp(i\delta_{\text{pot},c}+i\delta_{\text{pot},c'})\times\left[\delta_{cc'}+i\sum_{\lambda\lambda'}(\Gamma_{\lambda c})^{1/2}(\Gamma_{\lambda' c'})^{1/2}A_{\lambda\lambda'}\right], \quad (77)$$

where $\delta_{cc'}$ is the delta function, and the matrix inverse of $A_{\lambda\lambda'}$ is

$$(A^{-1})_{\lambda\lambda'}=(E_\lambda-E)\delta_{\lambda\lambda'}-i/2\sum_c(\Gamma_{\lambda c})^{1/2}(\Gamma_{\lambda' c})^{1/2}.$$

Using (75) and (77), we find

$$\delta\sigma_{\text{int}}\approx\frac{g_+}{4k^2}\times\left\{\sum_i\Gamma_{ni}\Delta E_i\frac{\Sigma_{i\neq j}\Gamma_j/\Delta E_j}{\Delta E_i^2+\frac{1}{4}(\Gamma_i+\Delta E_i\Sigma_{j\neq i}\Gamma_j/\Delta E_j)^2}\right\}+\text{similar term for the other spin } (g_-). \quad (78)$$

For the two levels of bismuth ($E_1=800$ eV and $E_2=2310$ eV), calculations using (78) give results which practically coincide with those in Table V. When all the known resonances of energy $E_j>0$ ($0<E_j<265$ keV; Ref. 17) are included, the inter-resonance interference term is $\Delta\sigma_{\text{int}}=0.108$ b for bismuth at an energy of order 10 eV (the total cross section for bismuth at this energy is $\sigma_{\text{tot}}=9.3$ b, i.e., 90 times larger).

However, it is very important that far from the resonances $\Delta\sigma_{\text{int}}$ for bismuth is practically independent of energy. This is confirmed by the results in Table V and also by analysis of (78), from which it follows that far from the resonances $\Delta\sigma_{\text{int}}\sim\Gamma_{nj}\Gamma_{j+1}/k^2\approx$const. The same can be said of Ref. 73, where the need to include inter-resonance interference was pointed out; there, for $\gamma^2=\Gamma_n/2kR$,

$$\Delta\sigma_{\text{int}}=R^2\sum\sum\frac{\gamma_i^2\gamma_j^2}{(E-E_i)(E-E_j)}\approx\text{const.} \quad (79)$$

However, the method by which $\Delta\sigma_{\text{int}}$ was obtained in that study is doubtful.[74]

In the Dubna study[46] the value of a_{ne} was determined by analyzing the value of $y=\sigma_{\text{tot}}(E)/4\pi-b^2_{\text{coh}}$, where b_{coh} is the coherent scattering length. The expression for y contains, in particular, the energy-independent term p_2, which is varied to obtain the best description of the experimental data. Since p_2 is independent of the energy, the introduction into σ_{tot} of the constant term $\Delta\sigma_{\text{int}}$ cannot affect the determination of a_{ne} in Ref. 46, although, of course, it slightly changes the analytic expression for p_2.

Using (56), we can obtain[75,76] an expression for the sum of p_2 and the inter-resonance interference term (78):

$$p_2+\Delta\sigma_{\text{int}}/4\pi=\frac{g_+g_-}{4}\left[\sum_+\frac{\Gamma_{ni}}{k_iE_i}-\sum_-\frac{\Gamma_{ni}}{k_iE_i}\right]^2+\frac{g_+}{4k^2}\sum_i\frac{\Gamma_{ni}}{\Delta E_i}\sum_{j\neq i}\frac{\Gamma_{\gamma j}}{\Delta E_j}+\text{similar term for the other spin } (g_-). \quad (80)$$

The second and third terms in (80) can be negative. Their signs depend on the resonance locations and strengths, and the energy at which the measurements are made. It is therefore possible for $p_2+\Delta\sigma_{\text{int}}/4\pi$ to be negative, as was found for bismuth in Ref. 46.

For even–even nuclei ($g_+=1$, $g_-=0$)

$$p_2+\Delta\sigma_{\text{int}}/4\pi=\frac{1}{4k^2}\sum_i\frac{\Gamma_{ni}}{\Delta E_i}\sum_{j\neq i}\frac{\Gamma_{\gamma j}}{\Delta E_j}. \quad (81)$$

For ^{208}Pb at a neutron energy of 1 eV, $p_2+\Delta\sigma_{\text{int}}/4\pi\approx6.3\times10^{-6}$ b/sr, and at energy 1970 eV, $p_2+\Delta\sigma_{\text{int}}/4\pi\approx1.4\times10^{-7}$ b/sr if only the known resonances at 507 keV and 1735 keV are taken into account. The inclusion of the resonance, found in Ref. 54, at negative neutron energy equal to -1900 keV of width $\Gamma_n^{(0)}=23$ keV has practically no effect. The contribution of this resonance to $p_2+\Delta\sigma_{\text{int}}/4\pi$ at a neutron energy of 1970 keV is less than 3×10^{-7} b/sr.

Regarding the value of $p_1 b_{\text{coh}}$, even at energy 1970 eV its value [see (53) and (55)] is less than 3×10^{-4} b/sr.

Therefore, the effect of resonance scattering on the value of a_{ne} determined for the ^{208}Pb sample at neutron energies up to 1970 eV can be neglected [$y=\sigma_{\text{tot}}/4\pi-b^2_{\text{coh}}A^2/(A+1)^2\approx0.01$ b/sr]. Equation (54) determining a_{ne} is simplified and for $\alpha_n\approx0$ (according to recent experimental data, $\alpha_n<0.5\times10^{-3}$ F[3]; see, for example, Ref. 49) takes the form

$$y=\sigma_{\text{tot}}/4\pi-b^2{}_{\text{coh}}A^2/(A+1)^2=(Z-F)^2a_{ne}{}^2 -2a_{ne}b_{\text{coh}}(Z-F)A/(A+1), \quad (82)$$

from which it follows that $\sigma_{\text{tot}}/4\pi=[b_{\text{coh}}A/(A+1)-a_{ne}(Z-F)]^2$, or

$$\sqrt{\sigma_{\text{tot}}/4\pi}=b_{\text{coh}}A/(A+1)-a_{ne}(Z-F). \quad (83)$$

From (83) we find

$$a_{ne}=1/(\sqrt{4\pi})[\sqrt{\sigma_{\text{tot}}(E_1)}-\sqrt{\sigma_{\text{tot}}(E_2)}]/[F(E_1)-F(E_2)]. \quad (84)$$

Using (84) to analyze the results reported in the summary study by Koester *et al.*,[49] we obtain the following (after introducing corrections into σ_{tot} for the aggregate state of the matter and Schwinger scattering) for the neutron energies $E_1=1.26$ eV and $E_2=5.19$ eV: $a_{ne}=(-1.58\pm0.30)\times10^{-3}$ F; for $E_1=1.26$ eV and $E_2=1970$ eV, $a_{ne}=(-0.26\pm0.15)\times10^{-3}$ F; and for $E_1=5.19$ eV and $E_2=1970$ eV, $a_{ne}=(+0.10\pm0.29)\times10^{-3}$ F. These results suggest that the value of σ_{tot} at $E_2=1970$ eV found in Ref. 49 is incorrect. Taking $\sigma_{\text{tot}}(1970)$ to be 11.525 b (instead of 11.479 b, as found in Ref. 49), we find $a_{ne}=(-1.59\pm0.15)\times10^{-3}$ F (for $E_1=1.26$ eV and $E_2=1970$ eV), and $a_{ne}=(-1.61\pm0.29)\times10^{-3}$ F (for $E_1=5.19$ eV and $E_2=1970$ eV), which is apparently close to the true value.

8. COMPARISON OF THE EXPERIMENTAL DATA WITH THE THEORY

Of course, from the viewpoint of the experimentalist, the question of the value of the scattering length a_{ne} is a purely experimental one. However, the available data should be compared with some of the modern ideas about the internal structure of the neutron. It seems to the present author that these ideas are best developed in quark models, whose foundations lie in the old Yukawa meson theory. It follows even from the latter that the virtual process $n\to p+\pi^-$ gives a negative tail in the neutron electric charge distribution (see Fig. 5). However, in all the old static representations of the nucleon it was unclear what the central part of the nucleon is. This problem was solved only within the framework of the modern ideas about the nucleon. The 1970s saw the birth of quantum chromodynamics (QCD), the quantum field theory of the strong interactions of quarks and gluons. In particular, QCD generalized the existing ideas about hadron structure. In contrast to the Maxwell equations, the QCD equations are nonlinear. For a few years afterwards, attempts were made to solve the QCD equations. In the absence of exact solutions it is natural to use phenomenological models which reflect the properties of QCD. One such model is the Cloudy Bag

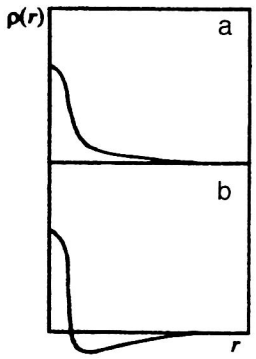

FIG. 5. Expected electric charge distribution in the nucleon: (a) proton, (b) neutron.

Model (CBM), proposed and developed by Thomas *et al.*[77] We note that the foundations of quark models of nucleon–bags were laid in the studies by theoreticians at the JINR, Dubna, performed in the mid-1960s. Bogolyubov apparently was the first to definitively formulate the "Dubna bag" model in 1967 (Refs. 78 and 79). This model represents a system of relativistic massless quarks moving freely inside a spherical volume. Further development of the Dubna ideas led to the creation of the MIT (Massachusetts Institute of Technology) bag model, whose main features then formed the basis of the CBM. One important defect of the MIT model was the fact that chiral symmetry is broken in it. Eliminating this required the inclusion of the interaction between quarks and the pion field at the bag surface. This hybrid model of a chiral bag (the CBM) was developed by Thomas *et al.* In this model the nucleon consists of a spherical static cavity of radius R filled with three massless valence quarks. The bag is surrounded by a cloud of negative pions which can be absorbed and emitted by the bag surface. The negative pions extend a distance of order $\hbar/m_\pi c>R$. Therefore, in the CBM the nucleon is not a point particle. The CBM gives a fairly successful description of the static properties of nucleons: the magnetic moments, form factors, charge radii, and so on. The calculations are performed in the static limit ($M\to\infty$), the nucleon is assumed to be at rest, and the corrections associated with nucleon recoil are introduced later. However, they only weakly affect the results (for example, in Ref. 80 they change the calculated neutron charge radius by no more than 6%).

The interaction of quarks with the pion field plays a decisive role in calculating the nucleon radius. For example, the radius calculated for the neutron in the MIT model, where there is no pion field, is zero. It should be noted that in the CBM it is the squared intrinsic charge radius of the neutron $\langle r^2_{E,\text{in}}\rangle_N$ which is calculated using the expression

$$\langle r^2_{E,\text{in}}\rangle_N=1/(e)\int\rho_N(\mathbf{r})r^2d\mathbf{r}, \quad (85)$$

where $\rho_N(\mathbf{r})=\rho^q_N(\mathbf{r})+\rho^\pi_N(\mathbf{r})$. The first term in the last expression describes the quark charge density, and the second is the same for the pion. Since the calculations are carried out for the nucleon–bag at rest ($M\to\infty$), the value (85) calculated in the CBM does not contain the Foldy term [see Ref. 80] due to Zitterbewegung, which, moreover, vanishes for

$M \to \infty$. It is also clear that (85) must be negative, because the region $r > R$ in which the negative pions are located gives a relatively larger contribution to the integral (85) than $r < R$. According to (85), which follows from the electric charge distribution in the neutron (see Fig. 5), it is simply impossible to obtain a positive value of $\langle r^2_{E,\text{in}} \rangle_N$. Therefore, the experimental data of Krohn and Ringo and of the Koester and Kopecky groups (see Table II) contradict the currently most well developed ideas about the structure of the neutron (see also Refs. 10, 75, 76, and 81). A positive value of $\langle r^2_{E,\text{in}} \rangle_N$ contradicts not only the CBM, but also other theories of the nucleon[82–84] which are also based on the Yukawa theory. It is practically impossible to obtain $\langle r^2_{E,\text{in}} \rangle_N > 0$ according to modern ideas.

The question sometimes arises of what should the theoretical results be compared with, $\langle r^2_{E,\text{in}} \rangle_N$ or $\langle r^2_{E,\text{in}} \rangle_N + \frac{3}{2}\mu_n(\hbar/Mc)^2$? This question was discussed already in the late 1950s and early 1960s within the Chew and Low model. Since all calculations of the nucleon radii are made in the approximation of a stationary (recoilless) heavy nucleon ($M \to \infty$), and in this case $(\partial G_{EN}/\partial q^2)_{q^2=0} \to \frac{1}{6}\langle r^2_{E,\text{in}} \rangle_N$, it appears to be correct to compare the results with $\langle r^2_{E,\text{in}} \rangle_N$, i.e., to subtract the Foldy amplitude from the measured value of a_{ne}.

CONCLUSION

The studies described above on the electromagnetic structure of the neutron have been carried out for more than 50 years now. However, there is still not complete understanding of even the neutron–electron scattering length, a quantity which would appear to be relatively simple to measure reliably in low-energy neutron physics. There are essentially two experimental values of this quantity: $\langle a_{na} \rangle = -1.58(3) \times 10^{-3}$ F and $\langle a_{ne} \rangle = -1.30(3) \times 10^{-3}$ F, although in this review I have tried to argue that the first value of a_{ne} is preferable. If the Foldy formula (8) is valid (and, in general, it is difficult to doubt its validity), then the first value of a_{ne} leads to a negative sign of the neutron squared intrinsic charge radius $\langle r^2_{E,\text{in}} \rangle_N$ at low energies. This does not contradict—indeed, it supports—the modern theoretical ideas about the neutron, i.e., static models of the neutron, for $M \to \infty$. If the second experimental value $\langle a_{ne} \rangle = -1.30(3) \times 10^{-3}$ F is correct, leading to $\langle r^2_{E,\text{in}} \rangle_N > 0$, it should be clearly understood that at present there are no theoretical ideas which can explain this fact. In this case it must be clearly stated either that the modern theoretical description of neutron structure at low energies is very far from accurate and is inconsistent with the experimental value of a_{ne}, or else that it is not completely correct, and then simply ignore this problem, as has recently been done in some studies (for example, Ref. 45).

The present review mainly contains the author's views on the problem of the neutron intrinsic charge radius. These views have been published in a number of journals (Phys. Rev., Rev. Mexicana de Física, Neutron News, Z. Phys., and elsewhere), reported at international conferences (Oaxtepec, Mexico; Santa Fe, USA; Trieste, Italy; Dubna, and others) and is supported by many physicists. It is to be hoped that new measurements and more accurate analysis of the experimental data already obtained will definitively solve this problem.

The author is grateful to G. S. Samosvat for useful discussions.

[1] P. A. M. Dirac, *The Principles of Quantum Mechanics*, 4th ed. (Clarendon Press, Oxford, 1958) [Russ. transl., Fizmatgiz, Moscow, 1960].
[2] S. V. Vonsovskiĭ and M. S. Svirskiĭ, Fiz. Élem. Chastits At. Yadra **28**, 162 (1997) [Phys. Part. Nuclei **28**, 66 (1997)].
[3] H. Feshbach, Phys. Rev. **84**, 1206 (1951).
[4] B. D. Fried, Phys. Rev. **88**, 1142 (1952).
[5] L. Foldy, Rev. Mod. Phys. **30**, 471 (1958).
[6] *Experimental Nuclear Physics*, edited by E. Segre (Wiley, New York, 1953) [Russ. transl., IL, Moscow, 1955].
[7] H. Frauenfelder and E. M. Henley, *Subatomic Physics* (Prentice-Hall, Englewood Cliffs, N.J., 1974) [Russ. transl., Mir, Moscow, 1979].
[8] M. N. Rosenbluth, Phys. Rev. **79**, 615 (1950).
[9] R. G. Sachs, Phys. Rev. **126**, 2256 (1962).
[10] Yu. A. Alexandrov, *The Fundamental Properties of the Neutron* (Clarendon Press, Oxford, 1992) [Russ. original, 3rd ed., Energoatomizdat, Moscow, 1992].
[11] G. G. Bunatian, V. G. Nikolenko, A. B. Popov *et al.*, Report E3-96-79, JINR, Dubna (1996).
[12] D. I. Blokhintsev, *Quantum Mechanics* (Reidel, Dordrecht, 1964) [Russ. original, 5th ed., Nauka, Moscow, 1976].
[13] E. Fermi and L. Marshall, Phys. Rev. **72**, 1139 (1947).
[14] A. I. Akhiezer and I. Ya. Pomeranchuk, Sov. Phys. JETP **19**, 558 (1949) [in Russian].
[15] V. Krohn and G. Ringo, Phys. Rev. D **8**, 1305 (1973).
[16] L. D. Landau and E. M. Lifshitz, *Quantum Mechanics: Non-Relativistic Theory*, 3rd ed. (Pergamon Press, Oxford, 1977) [Russ. original, 3th ed., Nauka, Moscow, 1974].
[17] S. V. Mughabghab, M. Divadeenam, and N. E. Holden, *Neutron Cross Sections*, Vol. 1 (Academic Press, New York, 1981); V. McLane, C. L. Dunford, and P. F. Rose, Vol. 2 (Academic Press, New York, 1988).
[18] W. Havens, I. Rabi, and L. Reinwater, Phys. Rev. **72**, 634 (1947); **82**, 345 (1951).
[19] K. Binder, Phys. Status Solidi **41**, 767 (1970).
[20] E. Melkonian, B. M. Rustad, and W. W. Havens, Jr., Phys. Rev. **114**, 1571 (1959).
[21] G. F. Chew and F. E. Low, Phys. Rev. **101**, 1579 (1956).
[22] G. F. Chew and F. E. Low, Phys. Rev. **101**, 1570 (1956).
[23] M. Friedman, Phys. Rev. **97**, 1123 (1955).
[24] H. Miyazawa, Phys. Rev. **101**, 1564 (1956).
[25] D. J. Hughes, J. A. Harvey, M. D. Goldberg, and M. J. Stafne, Phys. Rev. **90**, 497 (1953).
[26] O. Halpern, Phys. Rev. **133**, B579 (1964).
[27] Yu. A. Aleksandrov, Report 3-3442, JINR, Dubna (1967), p. 112 [in Russian].
[28] Yu. A. Aleksandrov, A. M. Balagurov, É. Malishevski *et al.*, Yad. Fiz. **10**, 328 (1969) [Sov. J. Nucl. Phys. **10**, 189 (1970)].
[29] L. Koester and H. Ungerer, Z. Phys. **219**, 300 (1969).
[30] Yu. A. Alexandrov, L. Koester, and G. S. Samosvat, Report E3-5371, JINR, Dubna (1970).
[31] Yu. A. Aleksandrov, T. A. Machekhina, L. N. Sedlakova, and L. E. Fykin, Yad. Fiz. **20**, 1190 (1974) [Sov. J. Nucl. Phys. **20**, 623 (1975)].
[32] Yu. A. Aleksandrov, A. M. Balagurov, G. S. Samosvat, and L. E. Fykin, Report R14-5358, JINR, Dubna (1970) [in Russian].
[33] G. E. Bacon, *Neutron Diffraction* (Clarendon Press, Oxford, 1955) [Russ. transl., IL, Moscow, 1957].
[34] Yu. A. Alexandrov and V. K. Ignatovich, Report E3-6294, JINR, Dubna (1972).
[35] Yu. A. Aleksandrov, J. Vávra, M. Vrana *et al.*, Zh. Éksp. Teor. Fiz. **89**, 34 (1985) [Sov. Phys. JETP **62**, 19 (1985)].
[36] Yu. A. Aleksandrov, J. Vávra, M. Vrana *et al.*, Pis'ma Zh. Éksp. Teor. Fiz. **42**, 200 (1985) [JETP Lett. **42**, 248 (1985)].
[37] A. S. Shumovskiĭ and V. I. Yukalov, Dokl. Akad. Nauk SSSR **252**, 581 (1980) [Sov. Phys. Dokl. **25**, 361 (1980)].
[38] A. S. Shumovskiĭ and V. I. Yukalov, Fiz. Élem. Chastits At. Yadra **16**, 1274 (1985) [Sov. J. Part. Nucl. **16**, 569 (1985)].
[39] Yu. A. Aleksandrov, Report R3-85-681, JINR, Dubna (1985) [in Russian].

[40] G. Glow and T. M. Holden, Proc. Phys. Soc. London **89**, 119 (1966).
[41] P. J. Brown, H. Cappelman, J. Deportes *et al.*, J. Magn. Magn. Mater. **30**, 243 (1982).
[42] L. Madhav Rao, in *Proceedings of the Fourth Intern. School on Neutron Physics* [in Russian], JINR, D3,4-82-704, Dubna (1984).
[43] L. Koester, W. Nistler, and W. Waschkowski, Phys. Rev. Lett. **36**, 1021 (1976).
[44] L. Koester, W. Waschkowski, and J. Meier, Z. Phys. A **329**, 229 (1988).
[45] S. Kopecky, P. Riehs, J. A. Harvey, and N. W. Hill, Phys. Rev. Lett. **74**, 2427 (1995).
[46] Yu. A. Aleksandrov, M. Vrana, J. Manrique Garcia *et al.*, Yad. Fiz. **44**, 1384 (1986) [Sov. J. Nucl. Phys. **44**, 900 (1986)].
[47] L. Koester, W. Waschkowski, and J. Meier, Z. Phys. A **337**, 341 (1990).
[48] Yu. A. Alexandrov, L. Koester, G. S. Samosvat, and W. Waschkowski, JINR Rapid Commun. No. 6[45]-90, JINR, Dubna (1990), p. 48.
[49] L. Koester, W. Waschkowski, L. V. Mitsyna *et al.*, Phys. Rev. C **51**, 3363 (1995).
[50] P. Prokofyevs, J. Tambergs, T. Krasta *et al.*, ISINN-2, E3-94-419, JINR, Dubna (1992), p. 220.
[51] Yu. A. Aleksandrov, Yad. Fiz. **37**, 253 (1983) [Sov. J. Nucl. Phys. **37**, 149 (1983)].
[52] Yu. A. Aleksandrov, Yad. Fiz. **38**, 1100 (1983) [Sov. J. Nucl. Phys. **38**, 660 (1983)].
[53] W. Triftshause, Z. Phys. **186**, 23 (1965).
[54] T. L Enik, L. V. Mitsyna, V. G. Nikolenko *et al.*, ISINN-3, E3-95-307, JINR, Dubna (1995), p. 238.
[55] Yu. A. Alexandrov, Neutron News **5**, No. 1, 20 (1994).
[56] Yu. A. Alexandrov, Rev. Mex. de Física **42**, 283 (1996).
[57] Yu. Z. Nozik, R. P. Ozerov, and K. Henning, *Structural Neutronography*, Vol. 1 [in Russian] (Atomizdat, Moscow, 1979).
[58] D. I. Svergun and L. A. Feigin, *Structure Analysis by Small-Angle X-Ray and Neutron Scattering*, edited by G. W. Taylor (Plenum, New York, 1987) [Russ. original, Nauka, Moscow, 1986].
[59] D. J. Horen, C. H. Johnson, J. L. Fowler *et al.*, Phys. Rev. C **34**, 429 (1986).
[60] G. Placzek, Phys. Rev. **82**, 392 (1951).
[61] G. Placzek, Phys. Rev. **86**, 377 (1952).
[62] J. R. Granada, Z. Naturforsch. Teil A **39**, 1160 (1984).
[63] S. Kopecky, P. Riehs, J. A. Harvey and N. W. Hill, in *Proceedings of the Intern. Conf. on Nuclear Data for Science and Technology*, Gatlinburg, Tennessee, 1994, Vol. 1, p. 233.
[64] J. M. Blatt and V. F. Weisskopf, *Theoretical Nuclear Physics* (Wiley, New York, 1952) [Russ. transl., IL, Moscow, 1954].
[65] I. S. Guseva, Preprints NP-27-1994, LIYaF-1969, Petersburg Nuclear Physics Institute, Gatchina (1994) [in Russian].
[66] Yu. A. Aleksandrov, G. S. Samosvat, J. Sereeter, and Ts. G. Sor, Pis'ma Zh. Éksp. Teor. Fiz. **4**, 196 (1966) [JETP Lett. **4**, 134 (1966)].
[67] J. Schmiedmayer, P. Riehs, J. A. Harvey, and N. W. Hill, Phys. Rev. Lett. **66**, 1015 (1991).
[68] P. Riehs, S. Kopecky, J. A. Harvey, and N. W. Hill, in *Proceedings of the Intern. Conf. on Nuclear Data for Science and Technology*, Gatlinburg, Tennessee, 1994, Vol. 1, p. 236.
[69] E. P. Wigner, Phys. Rev. **70**, 606 (1946).
[70] F. Vogt, Phys. Rev. **112**, 203 (1958).
[71] D. V. Adler and F. T. Adler, in *Proceedings of the Conf. on Breeding in Fast Reactors*, Argonne, 1963, ANL-6792, p. 695.
[72] A. A. Luk'yanov, *Structure of Neutron Cross Sections* [in Russian] (Atomizdat, Moscow, 1978).
[73] V. G. Nikolenko and A. B. Popov, Z. Phys. A **341**, 365 (1992).
[74] Yu. A. Alexandrov, Z. Phys. A **344**, 219 (1992).
[75] Yu. A. Alexandrov, Phys. Rev. C **49**, R2297 (1994).
[76] Yu. A. Alexandrov, Rev. Mex. de Física **42**, 263 (1996).
[77] A. W. Thomas, Adv. Nucl. Phys. **13**, 1 (1984).
[78] P. N. Bogolyubov, Report R2-3115, JINR, Dubna (1967) [in Russian].
[79] P. N. Bogolyubov, Ann. Inst. Henri Poincaré Phys. Theor. **8**, 163 (1968).
[80] A. W. Thomas, S. Theberge, and G. A. Miller, Phys. Rev. D **24**, 216 (1981).
[81] Yu. A. Alexandrov, Neutron News **5**, No. 4, 17 (1994).
[82] T. H. R. Skyrme, Nucl. Phys. **31**, 556 (1962).
[83] J. Nambu and G. Jona-Lasinio, Phys. Rev. **122**, 345 (1961).
[84] R. Bijker, F. Iachello, and A. Leviatan, Ann. Phys. (N.Y.) **236**, 69 (1994).

Translated by Patricia A. Millard